DESIGN AND FABRICATION OF A FEEDSTOCK DELIVERY SYSTEM FOR A 3 kW SOLAR GASIFICATION REACTOR

A THESIS

SUBMITTED TO FACULTY OF THE GRADUATE SCHOOL OF THE UNIVERSITY OF MINNESOTA

BY

Amey Kawale

IN PARTIAL FULFILMENT OF THE REQUIREMENTS FOR THE DEGREE OF MASTER OF SCIENCE

Dr. Jane H. Davidson, Adviser

August 2013

Acknowledgements

I would like to thank several people without whom this work would not be possible. First would be Dr. Jane Davidson, my advisor who invested her valuable time, effort, and instruction into this project. She was always accessible to ask a question, and weekly meeting with her resulted in continuous improvement of my work. I would also like to thank Dr. David Kittelson who gave his valuable inputs in my work. He suggested practical approaches whenever I had difficulties in my project.

In addition to above, I would like to thank Brandon Hathaway for his constant motivation and guidance. Despite of his busy schedule, he always spared time to have a discussion with me about project. I would also like to thank University of Minnesota's Initiative for Renewable Energy & the Environment (IREE) for providing financial funding to the project.

Finally there is my family, who always encouraged me to excel academically and even more so in life.

Abstract

In the present work, a feed delivery system for a solar gasification reactor was designed, fabricated and tested. The feedstock delivery system delivers the required amount of feedstock into the reactor which is a cavity of molten salt held at 1200K. The feed delivery rate was from 8±(0.4) gm/min to 15(±0.75) gm/min. The cellulose feed particles were of diameter 0.5mm. The feed delivery system is comprised of hopper, screw feeder, stepper motor and feed injector. The hopper was designed to store a feed supply needed for continuous one hour operation of the reactor at the feed delivery rate of 15(±0.75) gm/min. The screw feeder, which is rotated using a stepper motor, draws the feed particles from the hopper outlet and carries them in forward direction to the feed injector. The feed injector was designed using the principle of dilute phase pneumatic transport theory which takes into account the feed particle size and feed delivery rate. It is interfaced with the reactor and it carries the feed particles to the reactor cavity with the aid of a nitrogen gas flowing at a speed of 12 m/s. Cellulose feed particles tend to become mushy at temperature above 473 K; thus clogging the feed supply line. This clogging prevents the supply of feedstock to the reactor. To prevent clogging temperature of the feed supply line was kept below 473K using air jets impinging on the feed supply tubing. A Labview control scheme was designed to control the input to the Mass Flow Controllers (MFC) and to monitor and write the outputs from temperature and pressure sensors. Output signals were logged at a frequency rate of 1000 samples per minute.

TABLE OF CONTENTS

List of Tables

List of Figures

Nomenclature

Latin

A	Interface contact area, m^2
C	Radial clearance between screw and tubing, m
CAS	Critical applied stress, Pa
D	Screw diameter, m
D_c	Shaft diameter, m
d_p	Particle diameter, m
ff	Flow factor
F_{fw}	Frictional force per unit length between gas and injector, Nm^{-1}
F_{pw}	Frictional force per unit length between particles and injector, Nm^{-1}
F	Force on the screw flights, N
G	Mass flux of feed particles, kgm^{-2}
h	Natural convection heat transfer coefficnet,$Wm^{-2}K^{-1}$
H	Height of the hopper, m
L	Length of the feed injector, m
L_s	Slot length of wedge shaped hopper, m
$\dot{m}_{feed}$	Mass flow rate of feed out of screw feeder, kgs^{-1}
MFC	Mass Flow Controller
N_s	Effective speed of screw conveyer
p	Pressure, Pa
p_s	pitch of screw, m
p_1	Inlet static pressure at injector, Pa
p_2	Outlet static pressure at injector, Pa
Q_{act}	Actual throughput of screw conveyer, m^3s^{-1}
Q_f	Volume flow rate of gas, m^3s^{-1}
Q_p	Volume flow rate of particles, m^3s^{-1}
Q_t	Theoretical throughput of screw conveyer, m^3s^{-1}
Re	Reynolds number
R_e	Effective radius of screw conveyer, m
r	Radial distance from centerline, m
r_p	Particle radius, m

T	Temperature, K
TC	Thermocouple
t_s	Thickness of screw flight, m
U_{ch}	Choking velocity, ms^{-1}
U_f	Nitrogen gas velocity, ms^{-1}
U_p	Particle velocity, ms^{-1}
U_T	Terminal velocity, ms^{-1}
V_s	Screw Velocity, ms^{-1}
V_R	Relative velocity of particle w.r.t screw, ms^{-1}
V_L	Useful conveying velocity, ms^{-1}
V_{LT}	Theoretical conveting velocity, ms^{-1}
V_T	Rotational velocity of particle, ms^{-1}
W	Slot width of wedge shaped hopper, m

Greek

α	Helix angle, degree
α_e	Effective helix angle, degree
ε	Void fraction
ε_{ch}	Void fraction at choking
η_v	Volumetric efficiency of screw conveyer
δ	Angle of internal friction, degree
θ	Semi included angle of hopper, degree
λ	Helix angle of screw conveyer, degree
μ	Coefficient of kinetic friction
ρ_o	Bulk density, kgm^{-3}
ρ_f	Fluid density, kgm^{-3}
ρ_P	Particle density, kgm^{-3}
σ_C	Compacting stress, Pa
σ_D	Compacting stress, Pa
σ_Y	Yield stress, Pa
τ_w	Wall shear stress, Pa
ϕ_s	Surface friction angle, degree
ω	Angular velocity of screw, rad/s

Chapter 1

Product Design Specifications

1.1 Motivation

In the present work a feedstock delivery system for a prototype solar gasification reactor is designed, fabricated and characterized. It delivers feedstock to the reactor in the range of 8-15 gm/min. There were many technical challenges which were addressed while designing the feed delivery system. The reactor operates at around 1273K and thus one needs to take into account the effect of a high temperature on the feed delivery system. The system should be able to deliver feedstock with an accuracy of more than 95% in mass flow rate of the feedstock. Detailed objectives and challenges are given in section 1.3.

1.2 Reactor Description

Figure 1.1 shows a technical drawing of the prototype 3kW solar gasification reactor as well as location of the inlet ports for the feed. The reactor consists of a cavity and outer housing as shown in figure 1.2. Table 1.1 and table 1.2 give information about different features of the reactor with respect to figure 1.1 and figure 1.2 respectively. Concentrated solar radiation enters the cavity through an aperture and is absorbed by the walls of the cavity. The annular space between cavity and housing is filled with eutectic mixture of carbonate salts: sodium carbonate, potassium carbonate and lithium carbonate. The eutectic mixture of salts has a melting point of 670K. Feedstock is introduced through the feed inlet port along with a gasifying agent such as steam or carbon dioxide when molten salt temperature reaches 1200K resulting in flash pyrolysis and gasification reactions. The products of these processes are hydrogen and carbon monoxide, which together constitute synthesis gas.

Synthesis gas may be burned directly or further processed to liquid feeds such as methanol.

In figure 1.1, feed inlet ports are shown as feature # 4. The housing wall is indicated by # 5. The products of gasification reaction exit the reactor from outer tube (feature # 6). A drain tube (feature# 7) facilitates the removal of molten salt once the experiment is over. The cavity is shown as feature# 2 in figure 1.2.

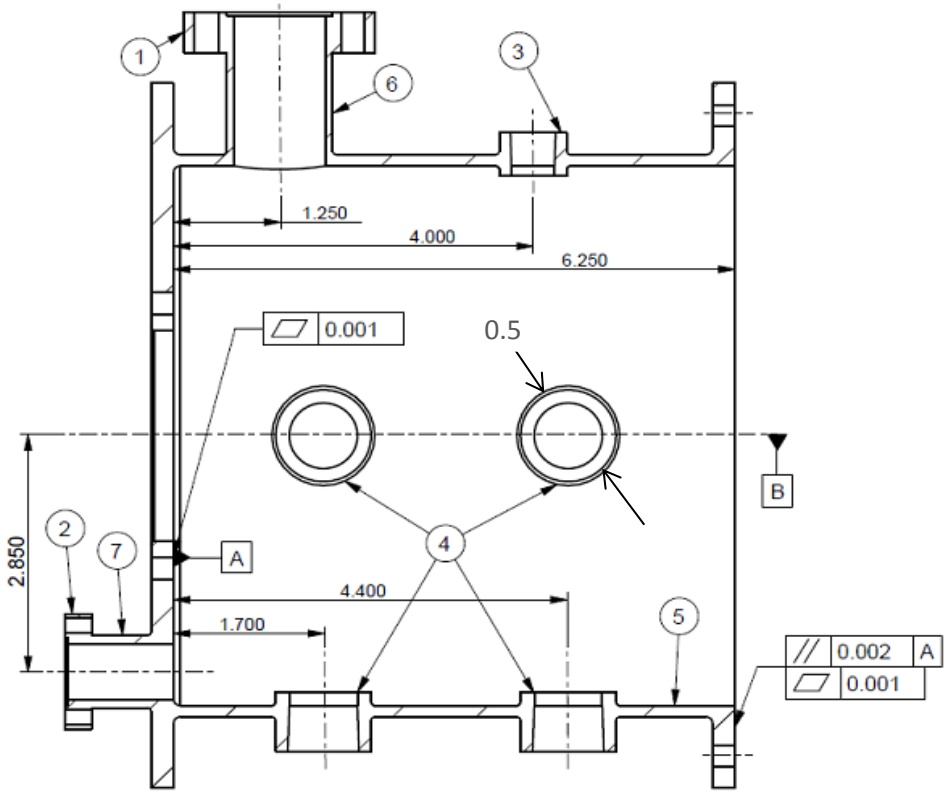

Fig 1.1: Location of feed inlet ports on the reactor (dimensions in inches) [1]

Table 1.1: Reactor components in figure 1.1 [1]

#	Feature	Description
1	Outlet flange	5.4cm CF flange
2	Drain flange	3.39cm CF flange
3	Probe ports	1×0.64cm NPT
4	Feed inlet ports	6×1.27cm NPT
5	Housing wall	16.51cm OD, 15.85cm ID
6	Outlet tube	2.54cm OD, 2.12cm ID
7	Drain tube	1.91cm OD, 1.30cm ID

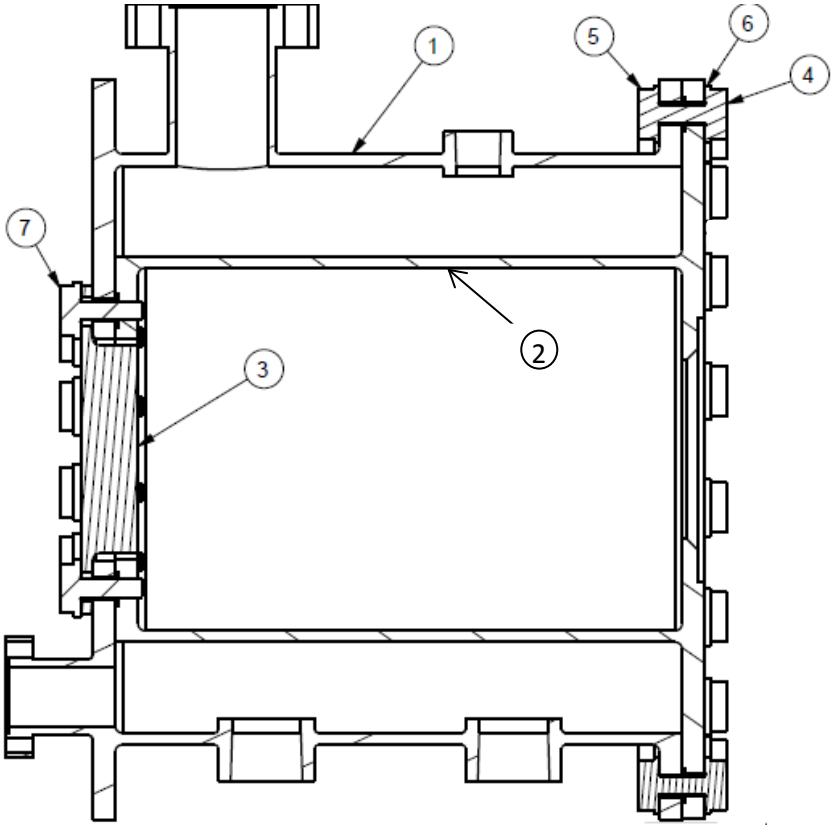

Figure 1.2: Side view of the reactor [1]

Table 1.2: Reactor components in figure 1.2 [1]

#	Feature	Quantity
1	Outer Housing	1
2	Cavity	1
3	Endcap	1
4	¼-20UNC-1” Bolt	18
5	¼-20UNC-Nut	18
6	¼-WSHR	54
7	¼-20UNC-3/4 CAPSCR	10

Microcrystalline cellulose (ARCOS Organics) was used as a feedstock material for the gasification reactor. The physical properties of the feedstock are given in table 1.3.

Table 1.3: Characteristics of the feedstock used for the gasification.

Material	Cellulose
Particle diameter	0. 5 mm
Bulk density	320 kg/m^3
Particle density	1200 kg/m^3

1.3 Product Design Specifications and Constraints

1. Feed Delivery Rate and Accuracy: The system should be able to deliver 8-15 gm/min of microcrystalline cellulose to the reactor with accuracy in feed delivery

mass flow rate more than 95%. In terms of volumetric feed rate, it translates to $(2.5\pm0.13)\times10^{-5}m^3$/min to $(4.7\pm0.24)\times10^{-5}m^3$/min.

2. Pressure: Molten salt present in the reactor needs to be prevented from flowing back into the feed delivery system. Thus the inlet pressure, P_{in} needs to be more than reactor outlet pressure and molten salt hydrostatic head. i.e., P_{in} > (101.325+3) kPa.

3. Feed Line Temperature: The feed delivery system is interfaced with the reactor operating at 1273K, thus conduction of heat occurs from the reactor to the feed delivery system. Feed particles begin to form system clogging tars if heated above 473K. Thus it is necessary to keep the temperature of the feed line below 473K.

4. Interface with Reactor: The feed injector (as shown in figure 1.3) should have 1.27cm (½") NPT fitting so that it can be interfaced with the feed inlet port.

5. Hopper Storage Capacity: The hopper should be able to supply feed material to the reactor continuously for one hour. Taking into account the upper range of feed delivery rate (15 gm/min) and bulk density of microcrystalline cellulose (from table 1.3), the hopper should have a minimum holding capacity of 28×10^{-4} m^3.

6. Screw Conveyer Size: Desired mass flow rates for the prototype reactor are of the order of 8-15 gm/min. Commercial screw feeders are available in large sizes and their outer diameter is larger than 5.08cm (2"). Use of such commercially available screw feeders would result in very low rotational speed of the order of 0.2-0.5 RPM in order to achieve desired feed rates due to their large volumetric throughput (more than $1.3\times10^{-4}m^3$/min). Controlling such a low RPM is difficult as well as it would lead to large uncertainty in feed rates. Thus, use of a commercially available screw feeder is not possible.

These constraints and other relevant parameters have been summarized in table 1.4.

Table 1.4: Operating parameters

Feed delivery rate	8-15 gm/min
Feed volume flow rate	$(25\times10^{-6} - 47\times10^{-6})$ m^3/min
Accuracy in feed delivery rate	> 95 %
Hopper storage capacity	>0.0028125 m^3
T_{feed_system}	< 473K
P_{in}	> 104.325 kPa

1.4 Design Concept and Sketch

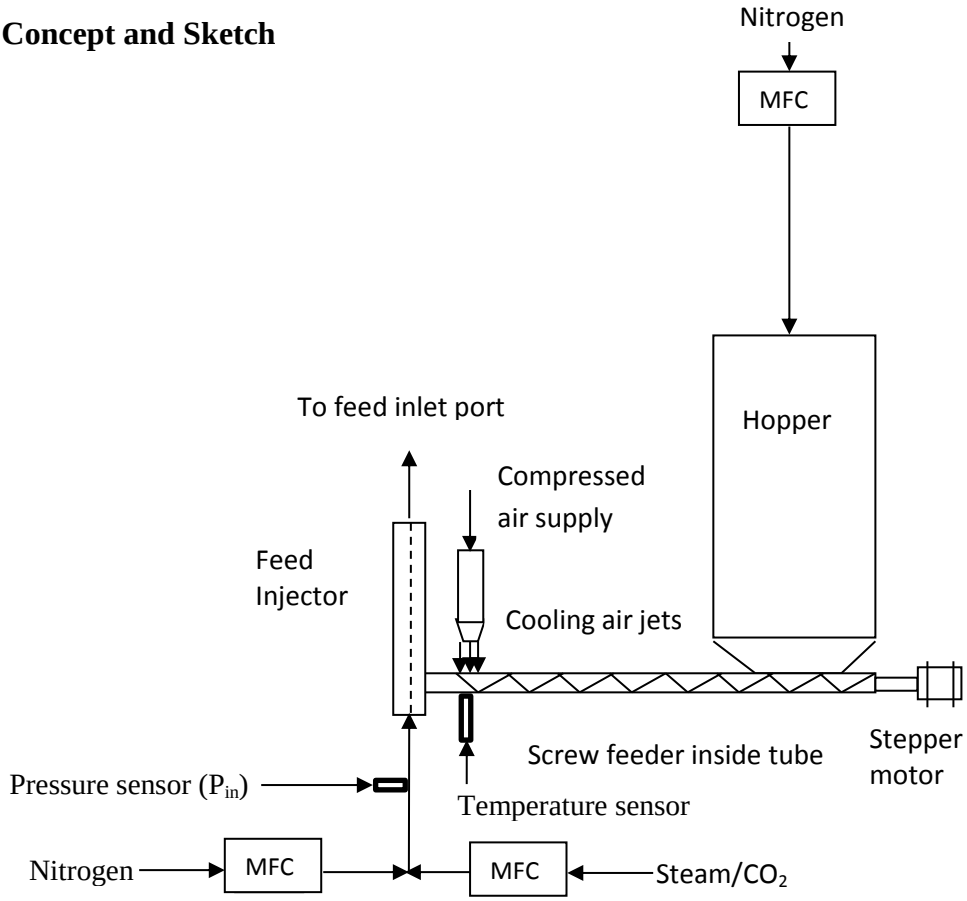

Fig 1.3: Schematic of a feed delivery system

Figure 1.3 shows a sketch of the concept of a feed delivery system. Detailed calculations and part drawings will be presented in consequent chapters. The feed system has a hopper for storage of a feedstock. Its volume is decided by the duration of an experiment and required mass flow rate of the feedstock to the reactor as given in table 1.4. From the hopper outlet, particles are carried in a forward direction towards the feed injector via a screw feeder enclosed in metal tubing. The screw feeder is driven using a stepper motor. A stepper motor is selected because it can accurately control the position of the screw feeder thus helping in precise calibration of mass flow rate of feed vs RPM of screw. The feed injector is connected to the reactor inlet using NPT fitting. The feed injector has two inlets and one outlet. One of the inlets receives feedstock particles from the screw feeder and other receives the high speed (12m/s) stream of inert gas (nitrogen) blended with steam or carbon dioxide. This high speed stream of gas carries the feed particles and gasifying agent up to the reactor. Gas speed and flow area are calculated using the principles of dilute phase pneumatic transport as described in chapter 4. The flow of an inert gas as well as of steam/carbon dioxide to the feed injector is controlled using a Mass Flow Controller (MFC). To maintain the pressurization criteria mentioned earlier, a small flow rate (300mL) of inert gas is used to pressurize the hopper. This approach ensures that the hopper pressure is more than feed injector pressure. The feedstock begins to react and produce system clogging tars if it is heated above 473K, thus the feed line is cooled using compressed air jets impinging at the feed line. To prevent the backflow of the molten salt into feed delivery system, a control scheme is implemented via Labview program and pressure measurement arrangement. The inert gas flow is variable but with a control scheme that prevents the flow being turned down so low that this pressure condition given in table 1.4 is violated. To ensure compliance with

the above norms, pressure sensors and temperature sensor are used. A pressure sensor (0-100 psia range) monitors the pressure upstream of the feed injector. If there is blockage in the feed injector, the pressure rises sharply and remedial measures are taken. A complete list of failure modes and remedial measures is given in Appendix C. A type-K thermocouple is attached at a diametrically opposite location of air jets. By varying the air jet flow rates, the temperature of feed line is kept below 473K.

1.5 Testing of the Feed Delivery System

Feed delivery system was tested on a mock up version of a reactor which consists of a Plexiglas column filled with water to a height which gives the same hydrostatic pressure (3kPa) head as that of the reactor filled with the molten salt. This system is used to visualize the feed delivery system in operation and to verify that the control scheme can keep liquid from flowing back into feed system. Detailed testing procedure is described in chapter 6.

Chapter 2

Survey of Different Types of Hoppers and Conveyers

2.1 Introduction

Whether for direct combustion, gasification, pyrolysis, or other biomass processes, a common critical problem is how to feed the biomass into the reactor [2]. The feeding system might clog partially, leading to a non-uniform flow of the feed material required for the process. The biomass particles themselves vary greatly in size and shape. Frequently they have reasonable moisture content, leading to the sticking of the feed particles to the feed supply line. They also tend to be compressible and pliable. Thus material handling is very important aspect of successful feed delivery system. Selection of an appropriate conveying system depends upon many factors such as type and quantity of bulk material, length of transportation, time available for transportation etc. The American Conveyor Equipment Manufacturer's association (CEMA) defines about 80 different types of conveyors. Some of the widely used are belt conveyors, screw conveyors, chain conveyors.

2.2 Types of Screw Feeders

The conveying component of a feed delivery system, a screw feeder/auger was selected after careful consideration of the options for conveying solid material in loose particulate form. It has simple structure, low cost, accurate throughput control, high volumetric efficiency and low cost of maintenance. It is an effective conveying devices for free flowing or relatively free flowing bulk solids and its output can be accurately calibrated as a function of rotational speed. Screw feeders have been popular devices among agricultural industry for conveying farm products. Thousands

of portable units have been used to move or elevate grains into and out of storage bins [3]. As one aspect of increased farmstead mechanization, many auger conveyors are being installed as integral parts of continuous-flow systems. The performance of a screw conveyor, as characterized by its capacity, volumetric efficiency, and power requirements, is affected by the conveyor geometry and size, the properties of the material being conveyed, and the conveyor operating parameters such as the screw rotational speed and conveying angle [4]. As shown in figure 2.1, the screw feeder basically consists of a shaft and helical flights. The flight is a continuous one piece helix shaped from a flat strip of steel welded onto the shaft. Shaftless screw feeders are also available. The flights are defined by type of shape and type of pitch. The flights are shaped to achieve better control on feeding for given material. Table 2.1 gives description of different types of screw flights. Pitch of the flight is the distance between two identical points on adjacent flights. Table 2.2 describes different types of pitch.

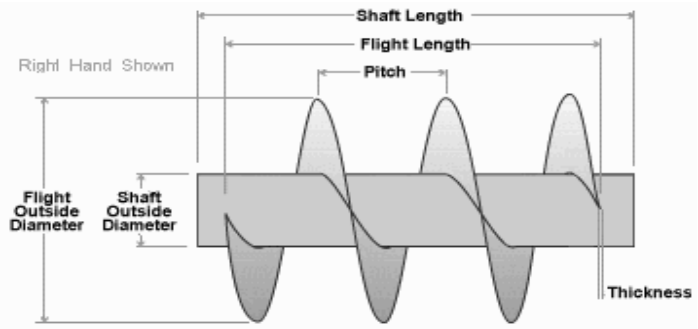

Figure 2.1: Screw feeder [5]

Table 2.1: Types of flights [6]

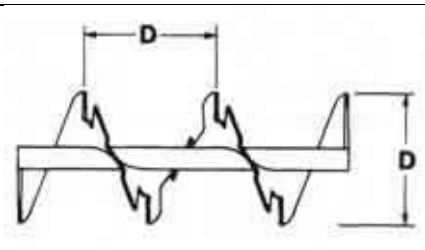	*Cut flights:* Flights are notched at regular intervals to allow mixing and agitation of the material, particularly materials which tend to pack. It is mostly used for light, fine, granular or flaky material.
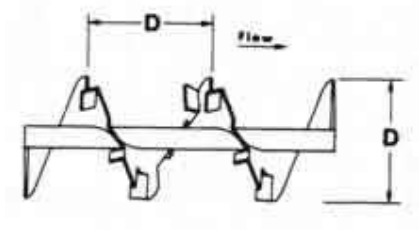	*Cut and Folded flight:* Flights have folded segments which act as lifting vanes and spill the material. These flights are excellent for heating, cooling or aerating light substances.
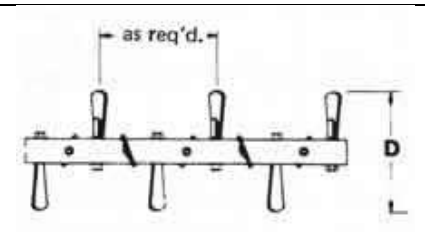	*Paddles flights:* Flights have blades mounted on the shaft. Paddle flights are used when more than one material is conveyed and it is desired to mix the feed.
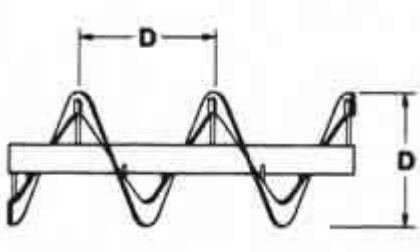	*Ribbon flights:* Flights have continuous helical structure and secured to the pipe by lugs. Ribbon flights are used for conveying sticky, gummy or viscous substances.

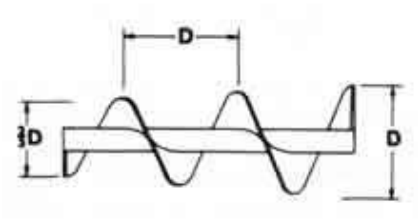	*Tapered, Standard Pitch, Single Flight:* Screw flights increase from 2/3 to full diameter along the axis of the rod. These flights aid uniform withdrawal of material.

Table 2.2: Types of pitch [6]

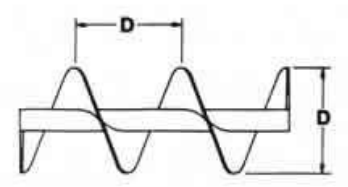	*Standard Pitch:* Pitch of screw is same as that of screw diameter. The standard pitch is suitable for a wide range of materials in most conventional applications.
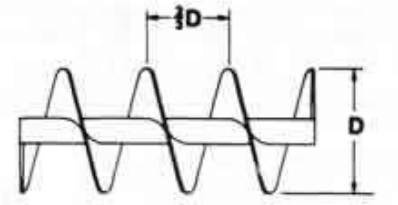	*Short Pitch, Single Flight*: Flight pitch is reduced to 2/3 diameter. It is recommended for inclined or vertical applications.
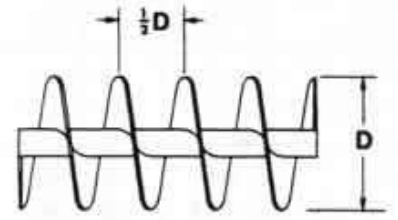	*Half Pitch, Single Flight:* Similar to short pitch, except pitch is reduced to 1/2 standard pitch. It is useful for vertical or inclined applications and for handling extremely fluid materials.

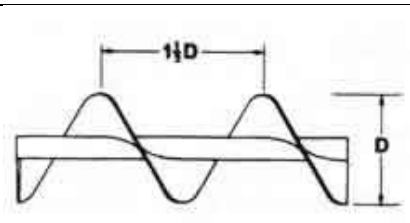	*Long Pitch, Single Flight:* Pitch is equal to 1.5 diameters. It is useful for rapid movement of very free-flowing materials.
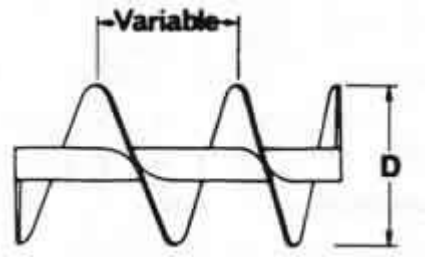	*Variable Pitch, Single Flight:* Flights have increasing pitch and are used in screw feeders to provide uniform withdrawal of materials over the full length of the hopper opening.

Selection of the size of the screw feeder is a function of the characteristics of the bulk material to be conveyed. These characteristics include maximum particle size, bulk density, corrosiveness and flowability. CEMA [7] has classified materials into four different classes as listed in table 2.3.

Table 2.3: Classification of Materials [7]

Class	Description	Example
1	Light, free flowing, non-abrasive	wheat, rye, shelled corn
2	Non-abrasive materials which are less free flowing .It is mostly small lumps mixed with fine material	baking powder, corn grits, pulverized coal
3	similar in size and	dry ashes, cement, salt,

	flowability as class 2, but more abrasive	charcoal
4	abrasive and poor flowability	furnace slag, alumina, dry sand

2.3 Hopper Design Theory

The hopper is used to store and supply feed material to the conveyer. The design of the hopper affects the rate of flow of the feed, how much of the stored material can be discharged and sets the effective holding capacity. [8]. Hoppers are categorized as mass flow hoppers or core flow hoppers. As shown in figure 2.2, in the mass flow hopper, all material in the hopper is in motion. Mass flow hoppers are smooth and steep (semi included angle is less than 20^{o}). Also in the mass flow hopper, the bulk density if the material remains constant. The "first-in–first-out" flow pattern of the mass flow hopper ensures a narrow range of residence times for solids in the hopper. On the other hand in the core flow hopper, only the core of the material is in motion; the bulk density of the material is not constant and the feed has a comparatively large residence time. A hopper might show mass flow behavior for one type of material and core flow for other type of material. For the feed delivery system, a mass flow hopper is preferable as it ensures smooth flow of the feed particles.

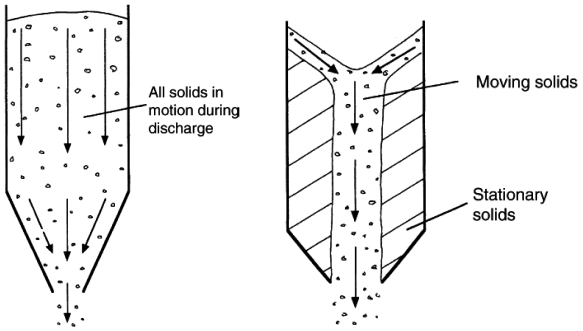

Figure 2.2: Mass flow hopper (left) and core flow hopper (right) [9]

The capability of a loose particulate solid to flow is termed "Flowability". It is an important parameter in hopper design defined by a flow factor, *ff*. It is the ratio of compacting stress to stress developed in the feed, as given by eq. 2.1. If the flow factor is high (more than 1 [10]), it results in low flowability. Parameters affecting flowability are feed material, hopper material and the geometry of hopper.

$$ff = \frac{\sigma_C}{\sigma_D} \tag{2.1}$$

The yield stress of the powder in the exposed surface of the arch is σ_Y known as the unconfined yield stress of the powder. If the stresses developed in the powder forming the arch are greater than the unconfined yield stress of the powder in the arch, flow will occur. The condition for the flow to occur is given by eq. 2.2.

$$\frac{\sigma_C}{ff} > \sigma_Y . \tag{2.2}$$

Figure 2.3 shows a plot of σ_Y vs σ_D along with powder flow function. There are three different possible cases.

Figure 2.3 presents three possible cases:

Case a: $\sigma_Y > \frac{\sigma_C}{ff}$ (No flow)

Case b: $\sigma_Y = \frac{\sigma_C}{ff}$ (Critical point)

Case c: $\sigma_Y < \frac{\sigma_C}{ff}$ (flow)

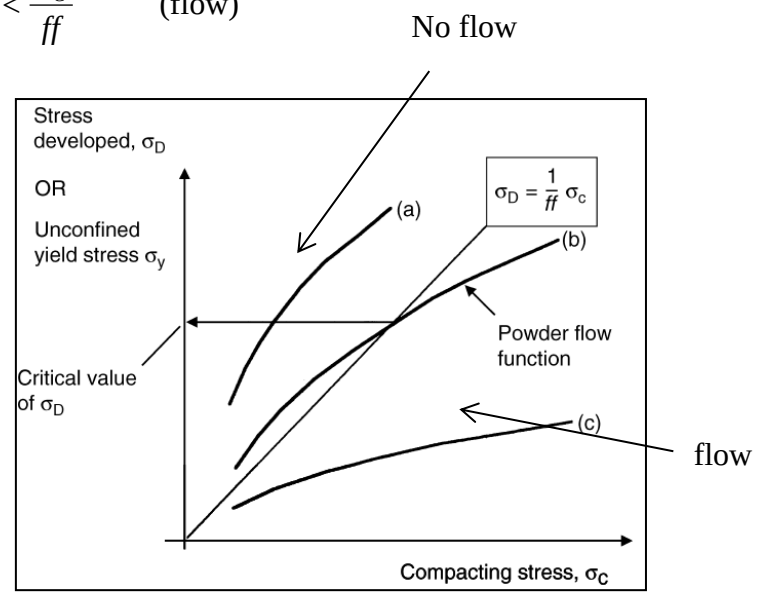

Figure 2.3: flow function [10]

Design charts for the mass hopper include a parameter called "the effective angle of internal friction". Mathematically it is the angle of the slope of the line through the origin that is tangent to the Mohr Circles at the critical point. The Mohr's circle represents the possible combinations of normal and shear stresses acting on any plane in powder under stress.

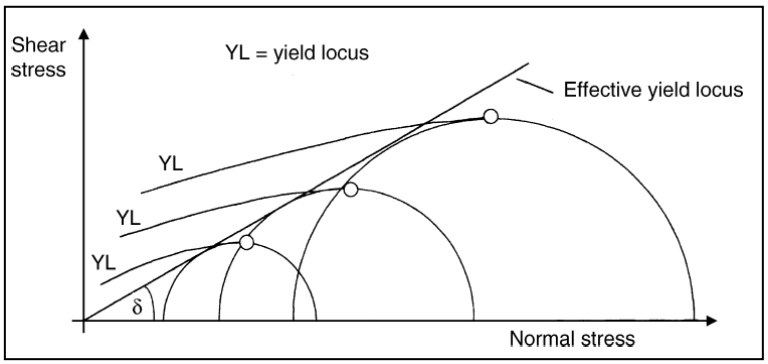

Fig 2.4: Effective angle of internal friction [10]

The angle of wall friction is given by $\tan^{-1}\mu$, where μ is coefficient of kinetic friction between material and hopper wall. It is determined using the tilting plate

method. In this method a thin layer of the bulk material is laid on to as horizontal plate made of the hopper wall material. The plate is then slowly tilted and the angle recorded at which the layer of bulk material begins to slide.

Jenike [9] has published charts for determining semi included angle for the wedge shaped (figure 2.6) mass flow hopper. If the material flow function *ff*, angle of internal friction and angle of wall friction are known then one can determine the semi included angle that would result in mass flow hopper for given material. Figure 2.5 shows the semi included angle for the wedge shaped hopper for different flow function, angle of internal friction (depends upon feed) and angle of wall friction combination (depends upon feed as well as hopper wall material).

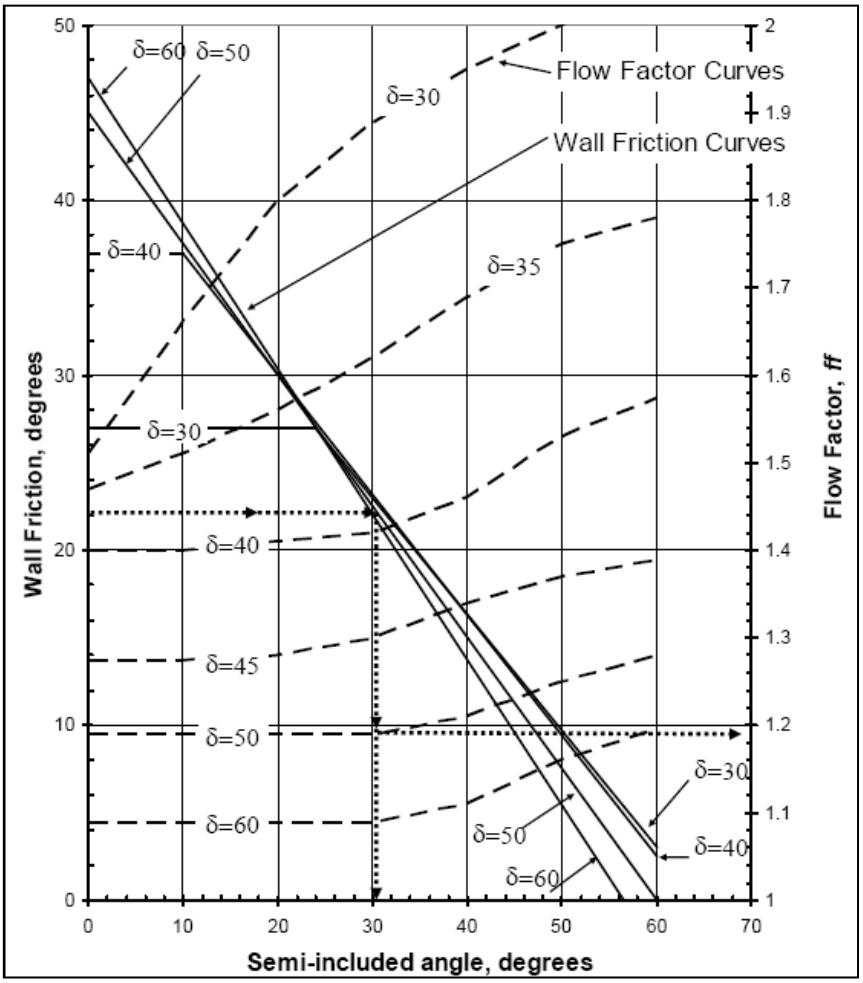

Fig 2.5: Flow factor [9]

Figure 2.6 shows the wedge shaped hopper with slot width W and slot length L. Semi included angle is determined using figure 2.5. The slot width, W is calculated as a function of H(θ), Critical Applied Stress (CAS) and bulk density of the feed, ρ_o. H(θ) is a function of semi included angle, θ (in degrees) and is determined using eq. 2.4.

$$W = H(\theta)\frac{CAS}{\rho_0 g} \tag{2.3}$$

$$H(\theta) = 1 + \frac{\theta}{180} \tag{2.4}$$

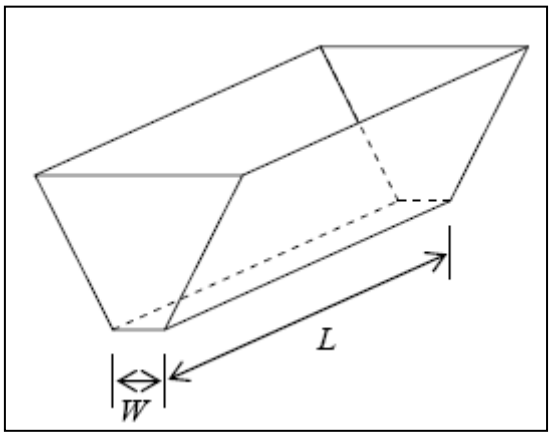

Fig 2.6: Wedge shaped hopper [9]

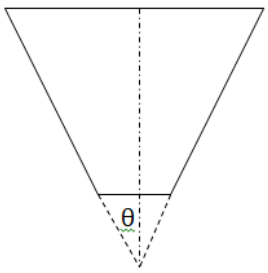

Fig 2.7: Semi included angle, θ.

2.4 Summary

This chapter provides an overview of screw conveyers and guidelines for selecting a screw conveyer based on a feed material. The advantages and

disadvantages of mass flow hopper and core flow hopper were presented. If feed material properties are known along with the hopper wall material properties, one can come up with the mass flow hopper geometrical parameters using Jenike's chart. These concepts and guidelines about screw feeder and hopper form the building blocks of the feedstock delivery system design and fabrication discussed in coming chapters.

Chapter 3

Design and Selection of Screw Feeder for Reactor

3.1 Design Objective

. The design objectives are summarized below.

1. To supply feed material to the reactor in the range of 8-15 gm/min.
2. To maintain an accuracy of 95% or more in feed delivery rate.

3.2 Design Theory and Calculations

Roberts [11] developed the theory to predict the performance of screw conveyors of any specified geometry.The theoretical maximum throughput Q_t, of an auger conveyer is obtained if the conveyer were running full with the particulate material moving purely in the axial direction. Auger conveyers are either with shaft and without shaft. The theoretical maximum throughput, Q_t, is given in equation 3.1.

$$Q_t = AwD^3 \tag{3.1}$$

$$A = \frac{1}{8}[(1+2\frac{C}{D})^2 - (\frac{D_c}{D})^2][\frac{p_s}{D} - \frac{t_s}{D}] \tag{3.2}$$

Where, C is the radial clearance between screw and tubing, D is the screw diameter, D_c is the shaft diameter, p_s is the screw pitch and t_s is the thickness of the screw flight.

The actual volumetric throughput of the auger, Q_{act} is less than theoretical and it is quantified by volumetric efficiency, η_v, given by,

$$\eta_v = \frac{Q_{act}}{Q_t} \tag{3.3}$$

The major factor determining volumetric efficiency is the rotational motion of the bulk material. As rotational speed increases, rotational motion decreases and volumetric efficiency increases [11]. Another factor affecting volumetric efficiency is the friction between the bulk material and the flow channel. It is characterised by Φ_s, the surface friction angle, which is given by arctan(μ_c) where μ_c is friction coefficient between bulk material and inner casing of tubing.

Figure 3.1 shows the velocity diagram for a particle in contact with the auger surface at a particular instant and location. Absolute particle velocity is resolved into two components,V_L which is the useful conveying velocity and V_T is rotational velocity. Roberts [11] found that V_T remains constant and does not vary with the radius. Screw velocity is indicated by V_s and V_R gives realtive velocity of the particle w.r.t screw. V_{LT} indicates theoretical conveying velocity. λ denotes the helix angle of the screw. Relation between V_L and V_{LT} is given by eq. 3.4.

$$\frac{V_L}{V_{LT}} = \frac{\tan\lambda}{\tan\alpha + \tan\lambda} \tag{3.4}$$

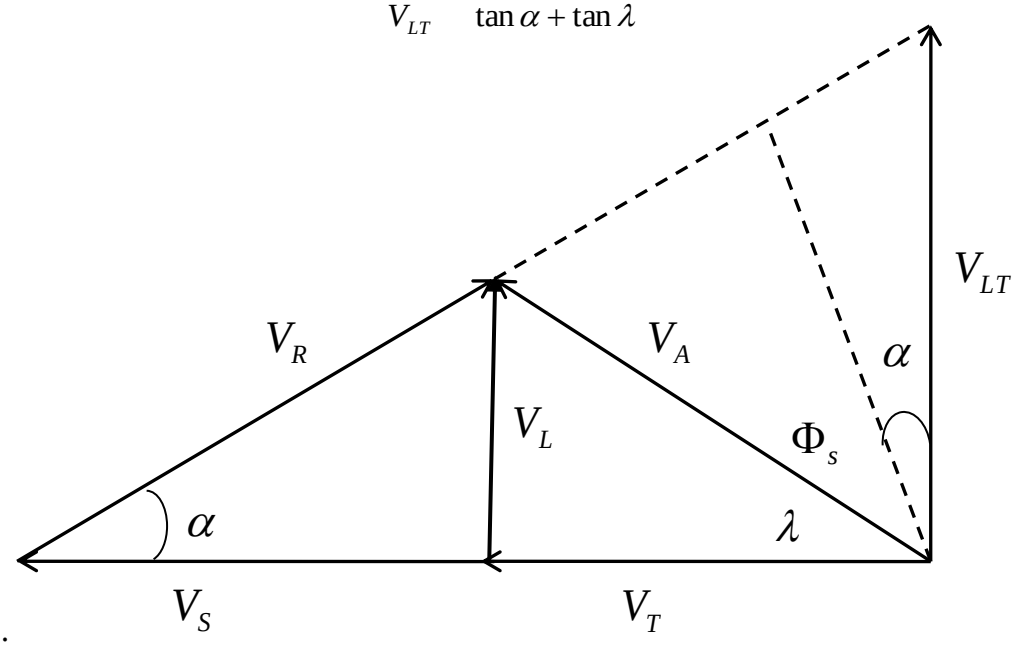

Fig 3.1: Velocity profile of a particle in screw feeder [11]

Location of bulk particles varies from shaft surface to periphery of the auger. Helix angle, λ varies along the radius of the auger. It is possible to define an effective radius, R_e to analyse forces and other useful parameters at effective radius instead of doing analysis along the auger radius and then integrating the results. R_e is expressed in terms of flight radius of the screw, R_o and shaft radius of the screw R_i. Effective helix angle, α_e is expressed in terms of screw pitch, p, screw flight diameter, D and effective radius, R_e. Effective radius, R_e and effective helix angle, α_e is given by eq.3.5 and 3.6 respectively.

$$R_e = \frac{2}{3}\left[\frac{R_o^3 - R_i^3}{R_o^2 - R_i^2}\right] \tag{3.5}$$

$$\alpha_e = \tan^{-1}\left[\left(\frac{p}{\pi D}\right)\left(\frac{R_o}{R_e}\right)\right] \tag{3.6}$$

Similarly, effective speed of screw is given by non-dimensional specific speed number, N_s. It is expressed in terms of angular velocity of the screw, w, screw flight diameter, R_o and acceleration due to gravity, g as given by eq. 3.7.

$$N_s = \frac{w^2 R_o}{g} \tag{3.7}$$

Volumetric efficiency of screw feeder, η_v is a function of effective helix angle, α_e and surface friction angle, Φ_s . η_v is given by eq. 3.8.

$$\eta_V = \frac{1}{\tan\alpha_e \tan(\alpha_e + \Phi_s) + 1} \tag{3.8}$$

Force analysis is carried out to determine force distribution on the screw feeder due to feed particles as well as to calculate torque which will enable to size the correct stepper motor. Force on the screw flights, F is given by eq. 3.9 [11]. F is a function of screw flight radius, R_o, screw shaft radius, R_i, screw pitch, p, bulk density of the feed material, ρ and friction coefficient between feed material and flow channel, μ_c.

$$F = 1.5\pi(R_o^2 - R_i^2)\, p\rho g\mu_c \tag{3.9}$$

Torque calculation is last step in determining the size of the stepper motor. Torque is calculated using eq. 3.10. Torque, T is a function of screw length, L_{sc}, screw pitch, p_s, force on the screw flights, F, effective radius of the screw, R_e, effective helix angle, α_e and surface friction angle Φ_s.

$$T = \frac{2}{3}\frac{L_{sc}}{p_s} F R_e \tan(\alpha_e + \Phi_s) \tag{3.10}$$

3.3 Selection of a Screw Feeder

Desired mass flow rates for the prototype reactor are of 8-15 gm/min. Since these are very small flow rates, use of commercially available screw feeders is not possible. Thus, a commercial screw feeder is substituted by a deep hole drill bit with 0.95 cm (3/8") outer diameter. Figure 3.2 shows the schematic of it. It has the screw flight diameter of 0.95 cm (3/8") and it is shaftless. It has the length of 30 cm (12").

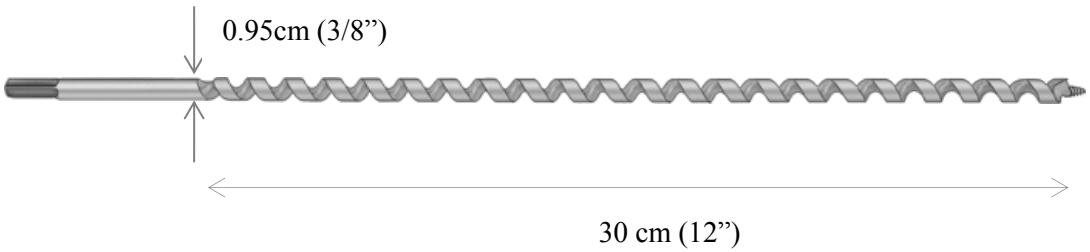

Figure 3.2: Deep hole drill bit [12]

We can now use the mathematical formulation described in section 3.2 to come up with different parameters associated with the screw feeder. Effective radius, R_e is calculated using eq. 3.5. For given screw, R_o=0.48cm, R_i=0 giving, $R_e = 0.64cm$.

Effective helix angle, α_e is calculated using eq. 3.6. For given screw, p_s=0.95cm, D=0.95cm, R_0=0.64cm, R_e =.0.64cm giving, $\alpha_e = 13.14^o$.

Φ_s is found to be 20^o using the tilting plate method described in chapter 2.

Volumetric efficiency, η_v of the screw feeder is calculated using eq. 3.8. For given screw, α_e=13.4^o, Φ_s=20^o giving, $\eta_V = 0.86$.

Theoretical volumetric throughput Q_t is found using eq. 3.1. For given screw, A=0.17, D=0.95cm giving, $Q_t = 1.62\times10^{-6}\,m^3/rev$. Taking into account the volumetric efficiency of 86%, actual throughput of the screw, Q_{act} is $2.84\times10^{-6}m^{3/}rev$.

For the feed rate of 12gm/min, the volumetric feed rate is $3.75\times10^{-5}m^3/min$. The required RPM is calculated by dividing volumetric feed rate by Q_{act} and is 13.2 RPM. However, the actual RPM required to maintain a feed rate of 12gm/min found by calibration (described in chapter 6) to be 24.5 RPM. Thus the actual volumetric efficiency of the screw feeder is less than the theoretical volumetric efficiency.

Torque, T is found using eq. 3.10 to be 10^{-2}N-m with specifications, L_{sc}=30.5cm, p_s=0.95cm, F=0.0012N, Re=0.64cm, α_e=13.4^o, Φ_s=20^o. Based on the above torque requirement, a stepper motor (NI NEMA 23) was selected which has holding torque of 1.98 Nm. Torque vs RPM characteristics for the selected stepper motor is given in fig 3.3. It is clear from figure 3.3 that, at operating speed around 22 RPM, the stepper motor can provide a torque of 0.9 N-m which is sufficiently larger than required torque of 0.01 N-m.

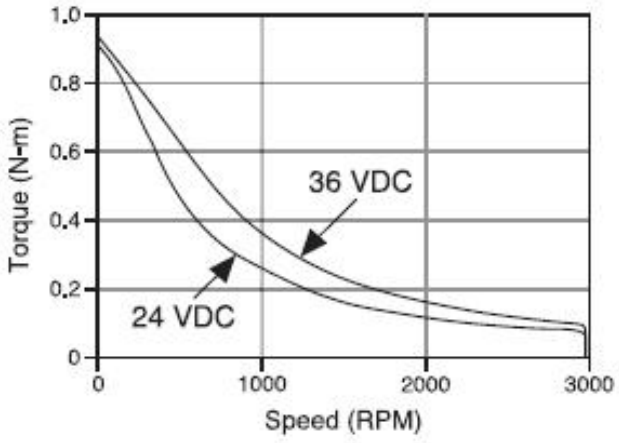

Fig 3.3: Torque vs speed characteristics for NI NEMA 23 stepper motor [13]

The motor torque is transmitted to screw feeder using a helical beam shaft coupling shown in figure 3.4. This coupling provides flexibility for parallel, angular and axial misalignments. Also it allows zero backlashes and never needs lubrication.

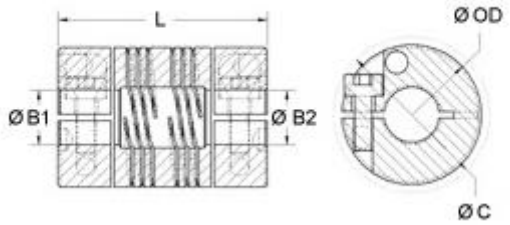

Figure 3.4: Helical shaft bean coupling with L = 3.81 cm,

$\Phi B1 = 0.64\text{cm}\,(0.25''),\ \Phi B2 = 0.95\,\text{cm}(3/8'')$

Fig 3.5 gives arrangement of stepper motor, coupling and a screw feeder shaft.

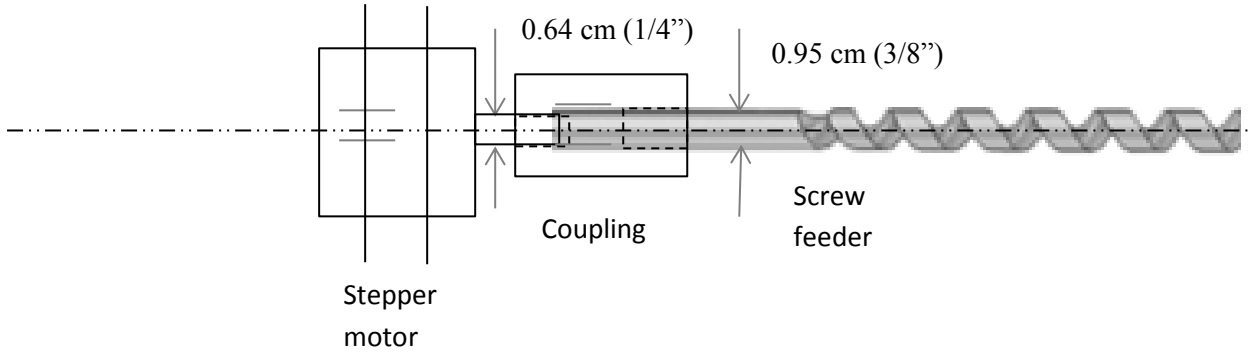

Figure 3.5: Arrangement of stepper motor, coupling and screw feeder

Figure 3.5 shows the arrangement of a stepper motor, shaft coupling and the screw feeder. Coupling has provision to hold two cylindrical shafts. One of the openings receives the 0.64 cm diameter shaft of a stepper motor and other receives 0.95cm diameter shaft of a screw feeder.

Chapter 4

Design of a Feed Injector

4.1 Design Objective

The feed injector is an important component of the feed delivery system. It carries the feed particles in a flow of nitrogen gas to the reactor. The design objectives for the feed injector can be broadly summarized as below:

1. To supply the feed material in the range of 8-15 gm/mins to the reactor using pneumatic transport.
2. To keep the volume flow rate of nitrogen as low as possible.
3. To interface with the feed port of the reactor which has 1.3 cm (1/2") NPT fitting.
4. To operate at temperatures $\leq$ 1200K.

4.2 Design Theory and Calculations

The feed injector was designed using the theory of dilute phase pneumatic transport in which gas is used as a transporting medium. Characteristics of dilute phase transport are given in table 4.1.

Table 4.1: Characteristics of dilute phase transport [14]

Gas velocity	>10 m/s
concentration of solid particles	< 1% by volume
low pressure drop	<5 mbar/m

Dilute phase pneumatic transport is limited to short route (less than 2m). Under dilute flow conditions the solid particles behave as independently and are fully suspended in the gas [14]. For successful transport of solid particles using pneumatic

transport, it is important to maintain gas velocities above a critical velocity, called the choking velocity, U_{ch}. The choking velocity depends on the solid feed rate. There is no theoretical expression for U_{ch} but there are number of empirical expressions. The most widely used is that given by Punwani et al.[15], and is given by eq. 4.1. In this equation U_{ch} is expressed as a function of void fraction at choking, ε_{ch}, flow channel diameter, D, terminal velocity of the feed particle, U_T and density of fluid used for pneumatic transport, ρ_f. In eq. 4.1, the unknowns are the choking velocity, U_{ch} and the void fraction at choking, ε_{ch}. Eq. 4.2 is a force balance between gravitational force on the feed particle and drag force on the feed particle and has two unknowns, choking velocity, U_{ch} and the void fraction at choking, $\varepsilon_{ch.}$ Eq. 4.1 and 4.2 are solved simultaneously for the choking velocity and the void fraction at choking. Terminal velocity, U_T of the solid particles in fluid is calculated using force balance given by eq. 4.3. In eq. 4.3, r_p is the solid particle radius, ρ_p is the particle density, ρ_f is the fluid density and μ_f is the viscosity of the fluid. .

$$U_{ch} = \varepsilon_{ch}\left(U_T + \left(\frac{2250D(\varepsilon_{ch}^{-4.7} - 1)}{\rho_f^{0.77}}\right)^{1/2}\right) \tag{4.1}$$

$$\frac{U_{ch}}{\varepsilon_{ch}} = U_T - \frac{G}{\rho_p(1-\varepsilon_{ch})} \tag{4.2}$$

$$U_T = \frac{2r_p^2(\rho_p - \rho_f)g}{18\mu_f} \tag{4.3}$$

Equation 4.1 has a constant 2250 which is dimensional and hence SI units must be used. Design of a dilute phase transport system involves selection of a combination of pipe size and gas velocity to ensure dilute flow and calculation of the resulting pipeline pressure drop. Since U_{ch} is based on an empirical expression, it does not predict exact choking velocity. Hence we need to be assuming some factor of safety while deciding gas velocities in pneumatic system. Bearing in mind the

uncertainty in the correlations for predicting choking velocity, a factor of safety of 1.5 or greater is recommended when selecting the operating gas flow rate [14].

Calibration of the feed delivery (as described in chapter 6) was carried out using the factor of safety of 1.5,i.e., U_f was kept $1.5U_{ch}$. However, as factor of safety was reduced from 1.5, it was found that pneumatic transport of the feed particles was successful till factor of safety of 1.2,i.e.,U_f was $1.2U_{ch}$. For a factor of safety less than 1.2, nitrogen gas flowing through the feed injector could not entrain all the feed particles. Thus throughout the calibration, 1.5 was used as a factor of safety.

The calculation of the pressure drop across the length of a feed injector is important as it gives estimation of the pumping power required. The pressure drop is composed of six different components. Figure 4.1 shows the schematic of feed injector for calculating pressure drops. Equation 4.4 gives the pressure drop calculation. In eq. 4.4, ε is the void fraction, ρ_f is the fluid density, U_f is the fluid velocity, ρ_p is the solid particle density, U_p is the particle velocity, L is the length of the feed Injector. F_{fw} is the frictional force per unit length between fluid and flow channel, F_{pw} is the frictional force per unit length between solid particles and the flow channel. $(U_f - U_p)$ represents the slip velocity between the particle and the fluid. For a feed rate of 15gm/mins, U_f is 13.14 m/s and U_p is 0.85 m/s, thus slip velocity is 12.3m/s. A complete solution is given in Appendix A.

$$p_1 - p_2 = \frac{1}{2}\varepsilon\rho_f U_f^2 + \frac{1}{2}(1-\varepsilon)\rho_p U_p^2 + F_{pw}L + F_{fw}L + \rho_p L(1-\varepsilon)g + \rho_f L\varepsilon g \qquad (4.4)$$

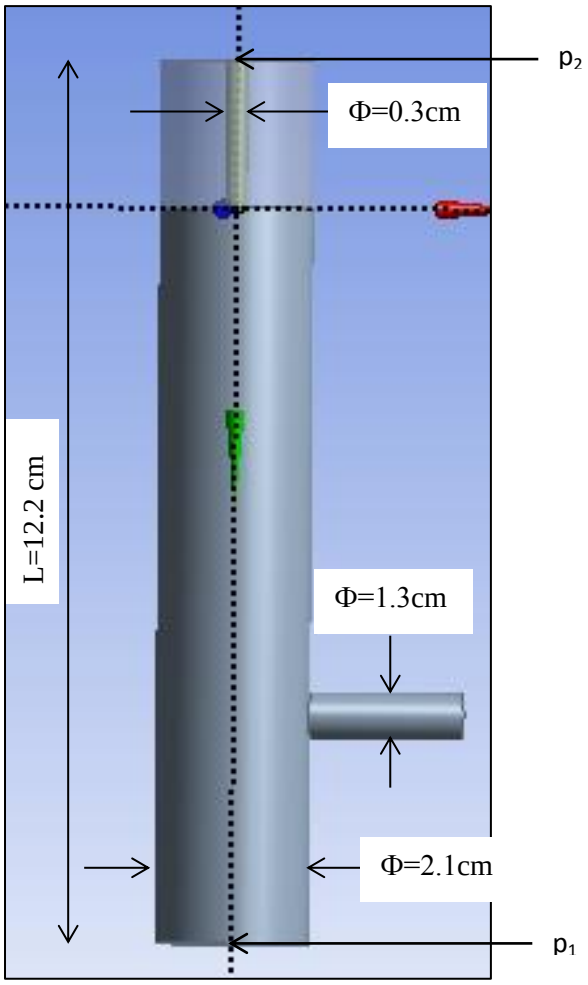

Figure 4.1: Schematic of feed injector for pressure drop calculations

Karman Nikuradse equation 4.5 [16] was used to find $F_{fw,}$ frictional force per unit length between fluid and flow channel. Eq. 4.5 gives wall shear stress, τ_w as a function of Reynolds number, Re, density of fluid, ρ_f and velocity of fluid, U_f. $F_{fw,}$ frictional force per unit length between fluid and flow channel is calculated using eq. 4.6.

$$\frac{\tau_w}{4\rho_f U_f^2} = (0.023)\,\mathrm{Re}^{-0.2} \tag{4.5}$$

$$F_{fw} = \frac{4\tau_w \pi}{D} \tag{4.6}$$

Figure 4.2 shows the variation of nitrogen gas velocity taking into account the factor of safety of 1.5 as a function of particle size. This velocity is a function of feed

particle size and increases with an increase in particle size. The feed particles used were of particle size of 0. 0005 m in diameter and gas velocity required for pneumatic transport of these particles is 12.47 m/s which translate to volumetric flow rate of 3.5 SLPM.

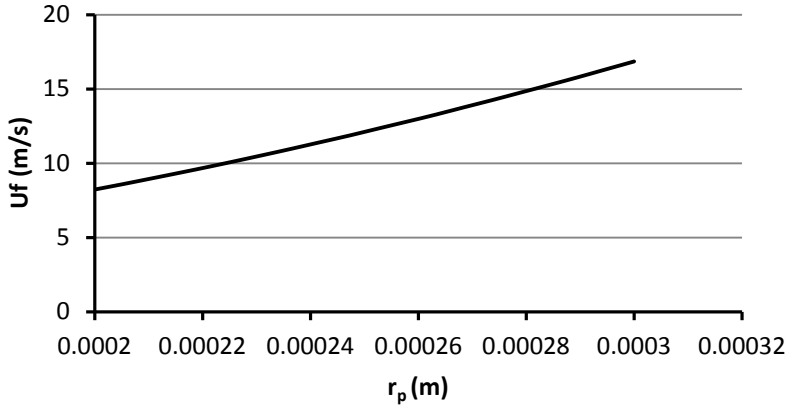

Fig 4.2: Variation of gas velocity as a function of particle radius

Figure 4.3 shows the variation of nitrogen gas volume flow rate through feed injector as a function of particle size. This volume flow rate is a strong function of feed particle size and increase with an increase in particle size.

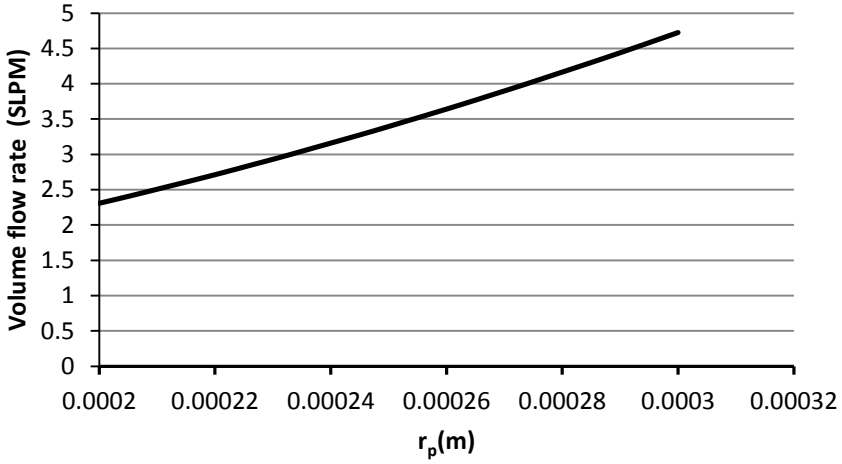

Fig 4.3: Volumetric flow rate of gas a function of particle radius.

Figure 4.4 shows the variation of pressure drop across the length of the feed injector as a function of gas velocity. The pressure drop increases with the increase in the gas velocity.

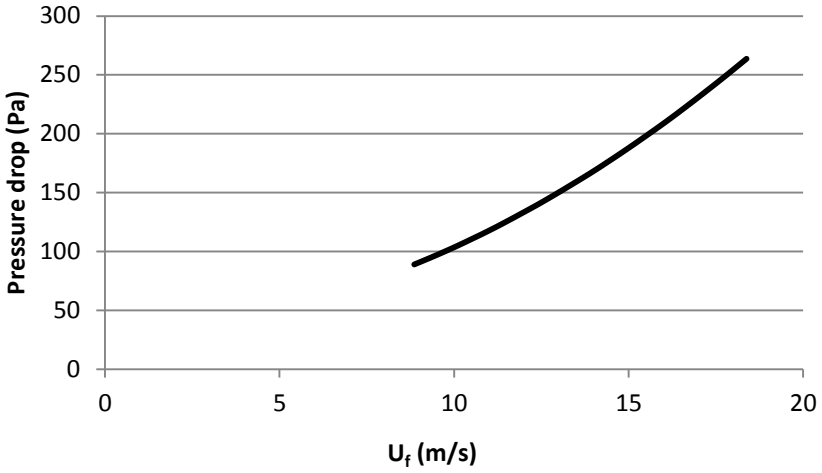

Fig 4.4: Pressure drop as a function of gas velocity

Figure 4.5 shows the pumping power (W) as a function of gas velocity. Pumping power is small due to very small flow passage area (7.3×10^{-6} m^2) of the feed injector.

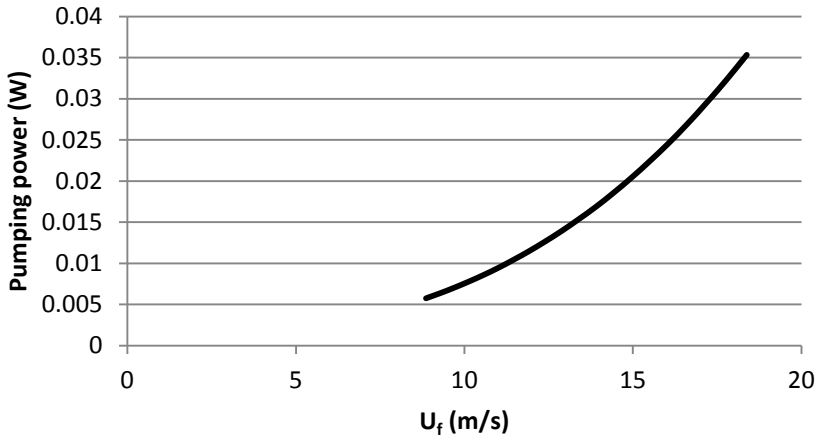

Fig 4.5: Pumping power as a function of gas velocity

Thermal and fluid flow analysis of the feed injector has been carried out using ANSYS™ to calculate the temperature distribution in the feed injector and the heat loss from the reactor via the feed injector. This heat loss decreases the thermal efficiency of a gasification reactor. The interface of the feed injector with the reactor is at 1200K and part of solar simulator energy input to the reactor is lost due to conduction of heat through the interface. Also as discussed in chapter 1, feed particles begin to clog if heated above 473K; thus simulation is required to predict the temperature distribution with the feed injector. Figure 4.6 shows the geometry of feed injector created in ANSYS. The geometrical dimensions are given in section 4.3. Since the material used for the manufacturing of the feed injector is SS316, its mechanical and transport properties are used in ANSYS model.

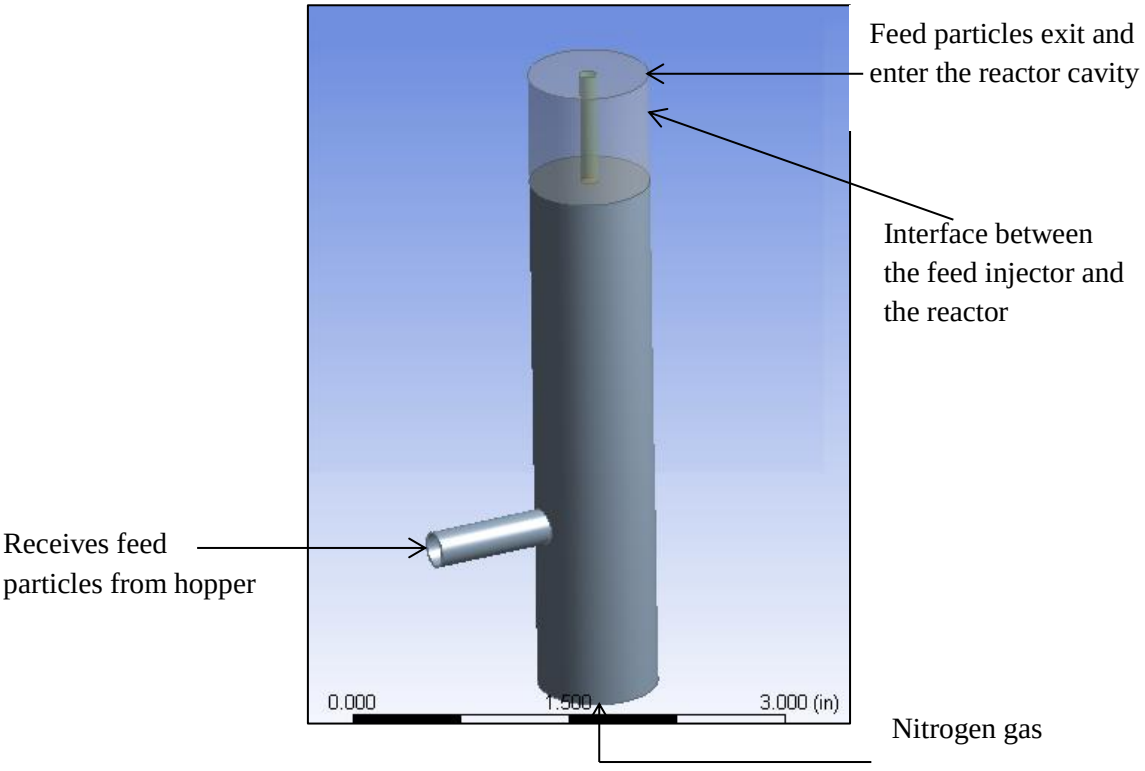

Fig 4.6: Geometry of the feed injector created in ANSYS

TheMulti Zone method was used to generate a mesh. It automatically created structured hex cells where possible and used tetrahedrons elsewhere. The type of

mesh used in the unstructured region was determined by the free mesh setting which were set to Tetrahedral. This automatic decomposition is a feature unique to Multi Zone which combines tetrahedral patch conforming and sweep mesh based on complexity of the geometry. It has 427503 numbers of elements and 496550 numbers of nodes.

Figure 4.7 shows the boundary conditions used to solve the 3 D steady state thermal energy problem. Gravity acts in negative z direction. The temperature boundary condition at the interface between injector and reactor is set at 1200K. Feed injector losses heat by convection to the ambient air; thus natural convection boundary condition is set at all exterior surfaces of the feed injector. Natural convection coefficient is set to 7 W/m^2 [17], and ambient temperature is set to 300K. Nitrogen gas speed and temperature at the feed injector inlet is set to 13 m/s and 300K respectively. Outlet pressure is set to 104.025 kPa as specified in section 1.3 of chapter 1.

Boundary conditions

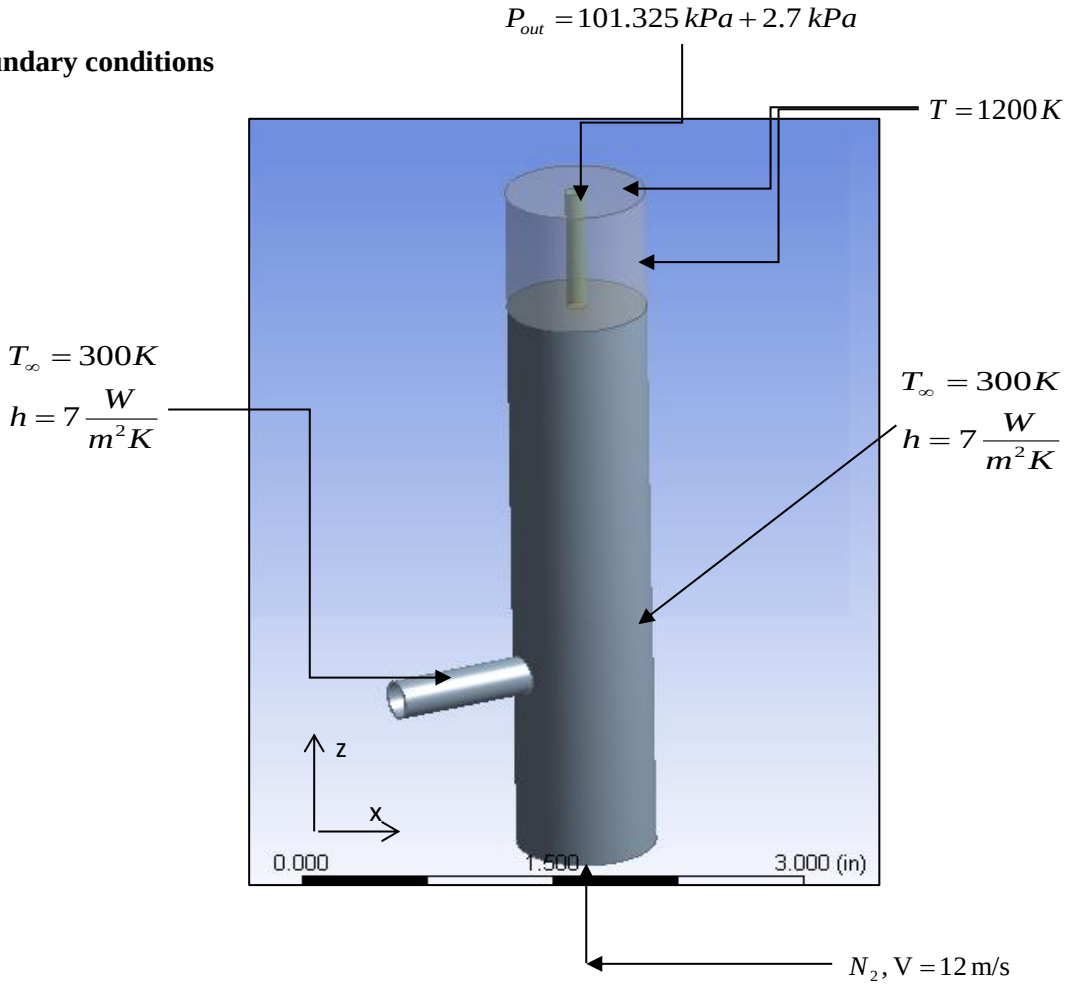

Fig 4.7: Boundary conditions

Results obtained from ANSYS simulation are presented in figures 4.8 and 4.9. Figure 4.8 gives the temperature distribution of the feed injector under boundary conditions depicted in fig 4.8. Figure 4.9 gives the distribution of average N_2 gas temperature along the length of the feed injector. This temperature distribution is used as an input to EES code (Appendix A) to solve for gas velocity, U_f.

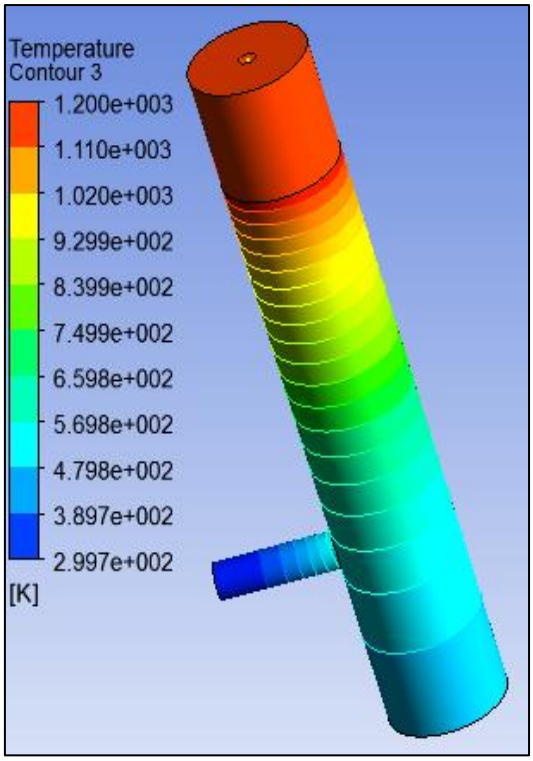

Fig 4.8: Temperature contours

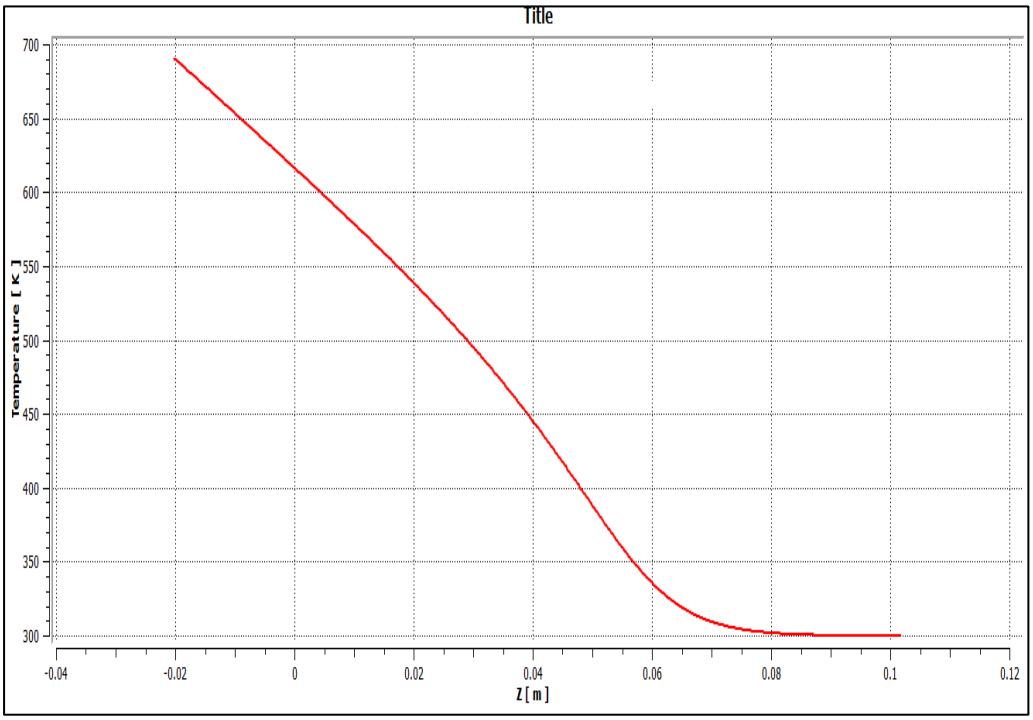

Fig 4.9: Distribution of average nitrogen gas temperature

Heat loss from injector-reactor interface

Average heat flux at the interface is 251.5 kW/m^2 .The interface is shown in figure 4.10. The interface area A is given by eq 4.7.

$$A = \frac{\pi}{4} D^2 + \pi D l \qquad (4.7)$$

The heat loss was calculated to be 0.43kW. It represents the conduction heat loss from reactor to feed injector. This heat loss decreases the thermal efficiency of a gasification reactor.

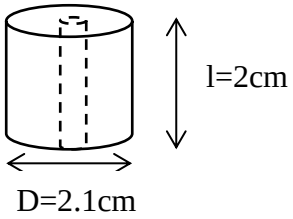

Fig 4.10: Interface between the feed injector and the reactor

Heat loss to the nitrogen gas

Nitrogen gas flowing through the feed injector is heated from 298K to the reactor temperature of 1200K. This heat input, $Q_{nitrogen}$ must be supplied by radiative input to the reactor. $Q_{nitrogen}$ is calculated using eq.4.8 and 4.9.

$$\dot{Q}_{nitrogen} = \dot{m}_f C_p (T_{reactor} - T_{room}) \qquad (4.8)$$

$$= V_f \dot{\rho}_f C_p (T_{reactor} - T_{room}) \qquad (4.9)$$

For this case, V_f is 5.83 10^{-5} m^3/s (3.5SLPM), ρ_f is 1.25kg/m^3, C_p is 1.13kJ/kg-K, $T_{reactor}$ is 1200K and T_{room} is 298K, giving $Q_{nitrogen}$ of 0.07kW.

4.3 Fabrication of the Feed Injector

Design of the feed injector was finalised taking into account the manufacturing feasibility. SS 316 is used for the fabrication of feed injector as it has excellent corrosion resistance. The diameter of the flow passage for the pneumatic

transport should be kept low to minimize the volume flow rate of nitrogen gas into the reactor. However, from a manufacturing feasibility point of view, 0.3cm (0.12”) was the lowest flow diameter possible as drills smaller than 0.3cm (0.12”) were too short and through hole of 12.2cm (4.8”) length (length of the feed injector as shown in figure 4.11) was not possible. The interfacing of the feed injector to the reactor is achieved through 1.3cm (½”) NPT threads. The interfacing of the feed injector with screw feeder tube is achieved through 1.3cm (½”) Swagelok™ tube to tube coupling. Other geometric parameters are chosen in such a way that they do not interfere with the reactor geometry. The detailed part drawings with dimensions (inches) are given in figure 4.11.

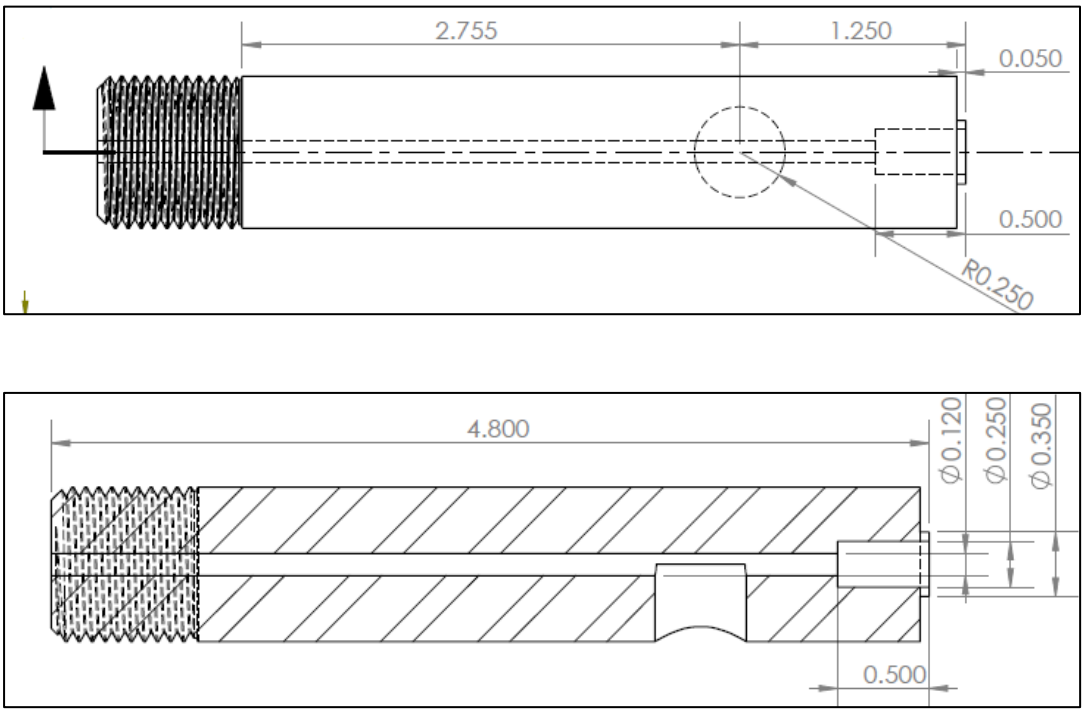

Fig 4.11: Geometry of feed injector (all dimensions are in inches).

Chapter 5

Design of Hopper

5.1 Design Objective

The hopper is used to store feedstock material. Design of the hopper affects the rate of flow of the feed material out of the hopper. The design objectives can be broadly summarized as below:

1. To store the 900gm of feed material.
2. To provide a means to monitor the level of feed inside hopper.
3. To provide a seal to prevent leakage of a gas used for pressurizing hopper.

5.2 Fabrication of the Hopper

Formulation described in section 2.3 of chapter 2 can be applied to the given feedstock material and the hopper material properties to obtain geometry required to produce a mass flow in the hopper. Material in consideration is cellulose powder. Hopper material is SS 316. The angle of wall friction Φ_s is determined experimentally using tilting plate method described in chapter 2. The angle of internal friction was found using [18].

Parameters associated with cellulose powder:

- The angle of wall friction, Φ_s: 25^o
- The angle of internal friction, δ: 35^o

Thus, from figure 2.5, we get:

- flow function, *ff*=1.6

- Semi included angle, $\theta = 20^0$

Width (W) for a hopper (figure 2.6) can be determined using eq. 5.1. In eq. 5.1, Width, W is calculated as a function of H(θ), Critical Applied Stress (CAS) and bulk density of the feed, ρ_o. H(θ) is a function of semi included angle, θ and is determined using eq. 5.2.

$$W = H(\theta)\frac{CAS}{\rho_0 g} \tag{5.1}$$

For hopper in consideration, H(θ) =1.14, CAS=800 Pa, ρ_o =320 kg/m^3,giving

$$W = 0.29m$$

$$H = 1 + \frac{\theta}{180} \tag{5.2}$$

Minimum width required for mass flow, W is about 29 cm. However due to geometric limitations described in chapter 1, it is not feasible. Figure 5.1 shows actual hopper assembly welded to tube. Sight glass is provided on top lid to see the level of feed. Gasket was used to seal the hopper. Chapter 6 discusses the result of leak test which was performed to check the effectiveness of gasket to prevent leakage.

Table 5.1: Geometrical parameter of hopper

Parameter	**Value**
Semi included angle	20^o
Slot Width,W	1.02cm (0.4")
Slot Length,L_s	10.2cm (4")
Height,H	31.5cm (12.4")

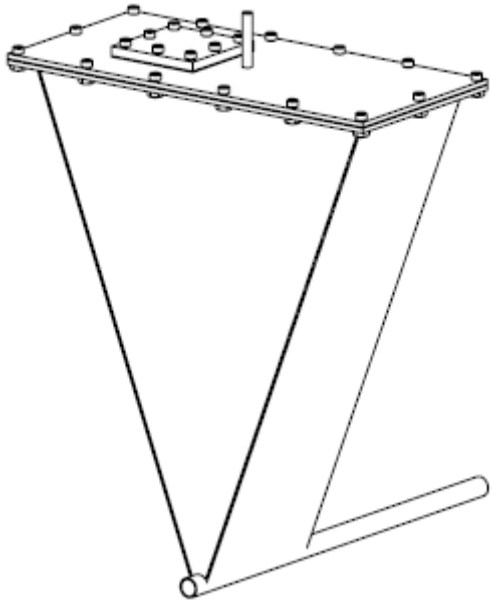

Fig 5.1: Isometric view of hopper

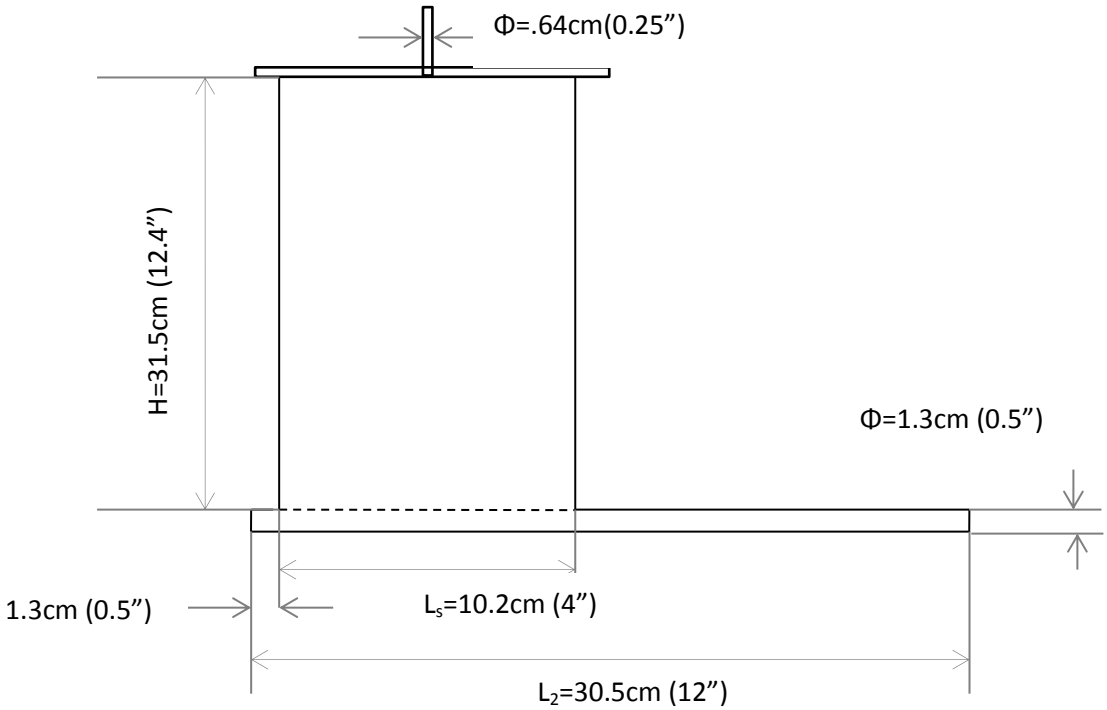

Fig 5.2: Side view of hopper

Chapter 6

Testing of the Feed Delivery System

6.1 Introduction

The intention of the testing was to calibrate the feed delivery system for feed delivery rate in the range of 8±(0.4) gm/min to 15±(0.75) gm/min. After successful testing, the feed system was ready to be connected to the gasification reactor. A Plexiglas structure was used to calibrate and evaluate the performance of the feed delivery system. Table 6.1 describes the various tests carried out. Figure 6.1 shows the schematic for testing. The Standard Operating Procedure (SOP) for feed delivery system is given in Appendix B.

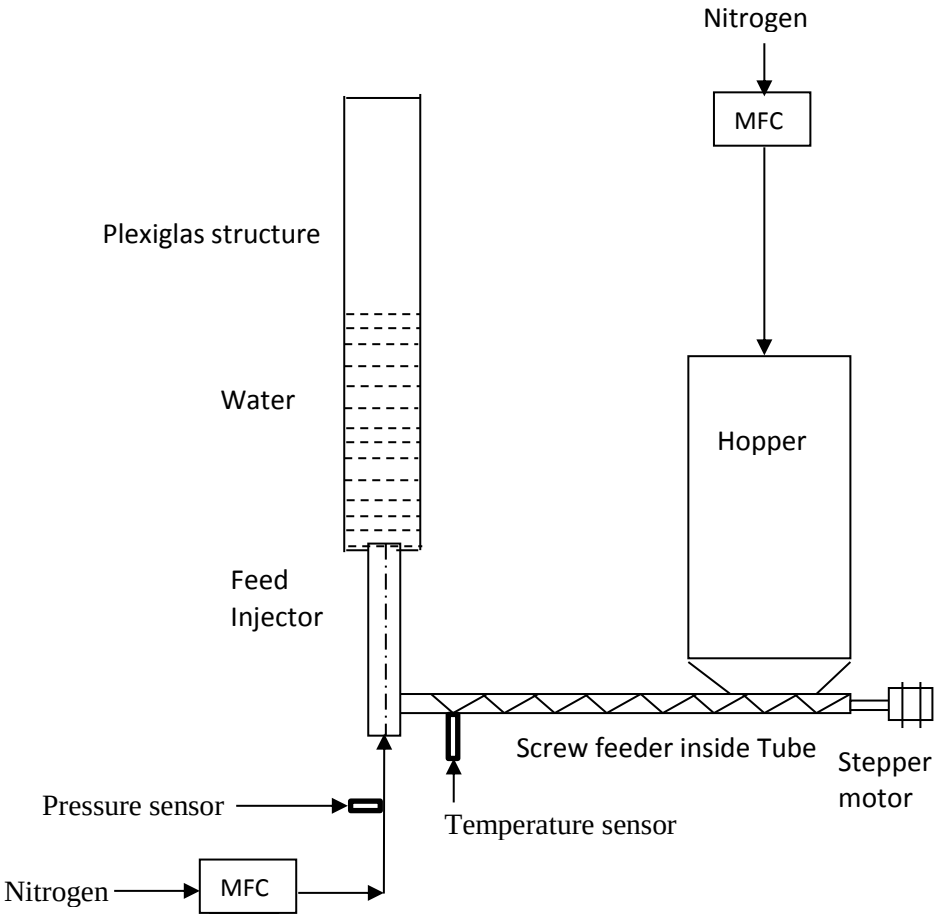

Figure 6.1: Schematic for testing feed delivery system

Table 6.1: Description of tests

Sr No.	Test Name	Objective	Procedure
1	Leak test	To identify leaks from feeder assembly, especially from hopper.	1. Pressurize the hopper 2. Apply soap solution at Gaskets, Swaglok fittings to check leakage.
2.	Dry test	To calibrate the feed delivery system	1. Attach feed injector to Plexiglas structure. 2. Start the feed injector gas flow and set it to 4.5 SLPM (based on dilute phase pneumatic transport calculations) use MFC 2. 3. Pressurize the hopper by setting flow rate to 300 SCCM (use MFC 3). 4. Start the stepper motor and set at 20 RPM. 5. Observe the system behaviour for any problems if any. 6. Run the system for 15 mins and collect the feedstock to measure mass flow rate.

			7. Repeat the procedure upto 30 RPM in steps of 1RPM.(i.e, 20,21,22 etc) 8. Carry out 3 repetitions for each RPM.
3.	Water column test	To observe if calibration obtained in test 2 changes by the presence of hydrostatic head	1. Repeat steps 1-3 from test 2. 2. Fill the acrylic column to desired height to produce hydrostatic head of 2.9kPa (this is same as that of produced by salt in the reactor. 3. Repeat steps 4-8 from test#2.
4.	High temperature dry test	To investigate if heated feed injector causes clogging of feedstock.	1. Wrap tape heater around feed injector and joint between screw inlet and feed injector. 2. Set the voltage such that temperature of 473K is achieved on feed injector surface. 3. Monitor temperature continuously.

			4. DO NOT attach acrylic column to feed injector. 5. Repeat steps 2-3 from test 2. 6. Vary the RPM form 20 to 30 in steps of 1. 7. Run the system for sufficient time (20-25 mins) to see if heated feed injector causes any clogging of feedstock. 8. Collect feedstock ejected out of feed injector in a pan.

6.2 Results of Tests

Results are summarized in table 6.2

Table 6.2: Results of tests

Sr No.	Test Name	Results
1	Leak test	Feed system could be pressurized to 7 psig.
2	Dry Test	Calibration results given in section 6.3
3	Water column test	Water did not flow back to the feed injector
4	High temperature dry test	No clogging observed

6.3 Calibration of the System

To accurately feedstock into the reactor, calibration of the screw feeder is carried out. During the calibration, the RPM of the screw was varied and at each RPM the mass of feed particles collected over the duration of 15 minutes is weighed to calculate the mass flow rate as a function of RPM. Three measurements were taken at each and the average value of mass flow rate is presented in the graph shown in figure 6.2. Measurements for mass flow rate are presented in table 6.3.

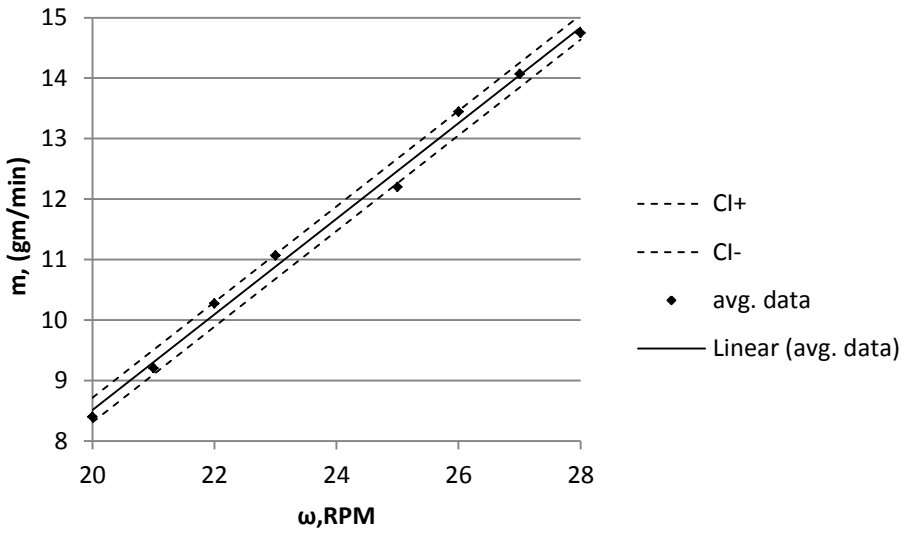

Fig 6.2: Calibration of the feed system

6.4 Uncertainty Analysis

Figure 6.1 shows the calibration graph for feed delivery system. Experimental data points as well as best linear fit line is shown. The upper and lower confidence intervals (CI+ and CI- respectively) are shown with the dotted line. Uncertainty in the data is calculated using LINEST function in Excel. It gives SEE (Standard Error of Estimate) which is a statistical measure of how well the best-fit line represents the data. This is, effectively, the standard deviation of the differences between the data points and the best-fit line. It provides an estimation of the scatter/random error in the data about the fitted line.

$$SEE = \left(\frac{\sum (y_i - y_{i,predcited})^2}{N-2} \right)^{1/2} = 0.18 \qquad (6.1)$$

$$CI(95\%) = \Delta y = \pm t(\alpha, \nu) SEE / \sqrt{N} = 0.20 \qquad (6.2)$$

Uncertainity in slope, $\Delta m = 0.07$

Uncertainity in intercept, $\Delta b = 2$

Taking into account the uncertainties in slope and intercept, we get $\dot{m}_{feed} = (0.79 \pm 0.07)RPM - (7.32 \pm 2) \quad ; 95\%\,\text{CI}$

Table 6.3: Calibration of the screw feeder

RPM	Reading 1 (gm/min)	Reading 2 (gm/min)	Reading 3 (gm/min)	Average (gm/min)
20	8.375	8.421	8.392	8.396
21	9.184	9.234	9.192	9.203
22	10.256	10.288	10.274	10.273
23	10.943	11.232	11.022	11.066
25	12.058	12.344	12.203	12.202
26	13.277	13.657	13.392	13.442
27	13.967	14.213	14.023	14.068
28	14.54	14.992	14.712	14.748

6.5 Reactor Testing

Once the feed delivery system was successfully tested using the tests described in section 6.2, it was tested with the reactor. For the reactor test, hopper was filled with an initial mass of 599.5g of cellulose powder. The reactor was heated up to 1150 K using solar simulator with a flow of 3.6 SLPM of nitrogen through the feed injector. Once molten salt reached 1150 K (monitored using Labview with type-K TC), CO_2 flow (gasifying agent) of 2 SLPM was turned on into the feed injector in addition to the N_2 (for pneumatic transport of feed particles) flow. The feed delivery system was turned on with the stepper motor being assigned a rotational velocity of

18 rpm. At this time the injector temperature was at a temperature of 98^{o}C, and it varied between 98^{o}C and 95^{o}C throughout the run time. The big pressure spike occurred six minutes after the feed was initiated, after which the feed seized up in the feedscrew shaft.

After the test run was over, the feed system was taken apart and it was found that the feed injector was actually not blocked in the vertical passage, but it was blocked in the side passage where the feedscrew comes in. The final mass of cellulose remaining in the hopper and feedscrew was 557.6g.

Based on the Labview data, it looks like the rising pressure in the reactor (due to the filters loading up with char/tar) caused the feed injector flow of N_2 to decrease to the point that entrainment of the feed particles was no longer possible. If N_2 flow going through the feed injector was not decreased, the feed system would have continued to run fine.

Chapter 7

Labview Control Scheme

7.1 Objective

Real time sensor output monitoring is very important during a test run. It enables the user to identify anomalous behavior if any. Also output from sensors needs to be continuously logged to a file in order to do the post processing of the data. Mass Flow Controllers (MFCs) need input signal from user to allow the required amount of gas flow through it. A Labview program is written in order to achieve above mentioned utilities. It communicates between different sensors and a computer. It also sends the input signal to the MFCs as given by the user. Table 7.1 lists various sensors and associated Labview program activity. The location of various sensors is shown in figure 7.2.

Table 7.1 Sensors and related Labview activity.

Sensor	# of sensors	Labview activity
Type K thermocouple	12	1. To monitor temperatures in realtime. 2. To record temperature data into a file
Absolute pressure sensor	2	1. To monitor inlet and outlet reactor pressures in realtime. 2. To record pressure data into a file.
Mass Flow Controller (MFC)	3	1. To set a setpoint for MFC. 2. To monitor the return signal continuously from MFC. 3. To record flow rates of gases into a file.

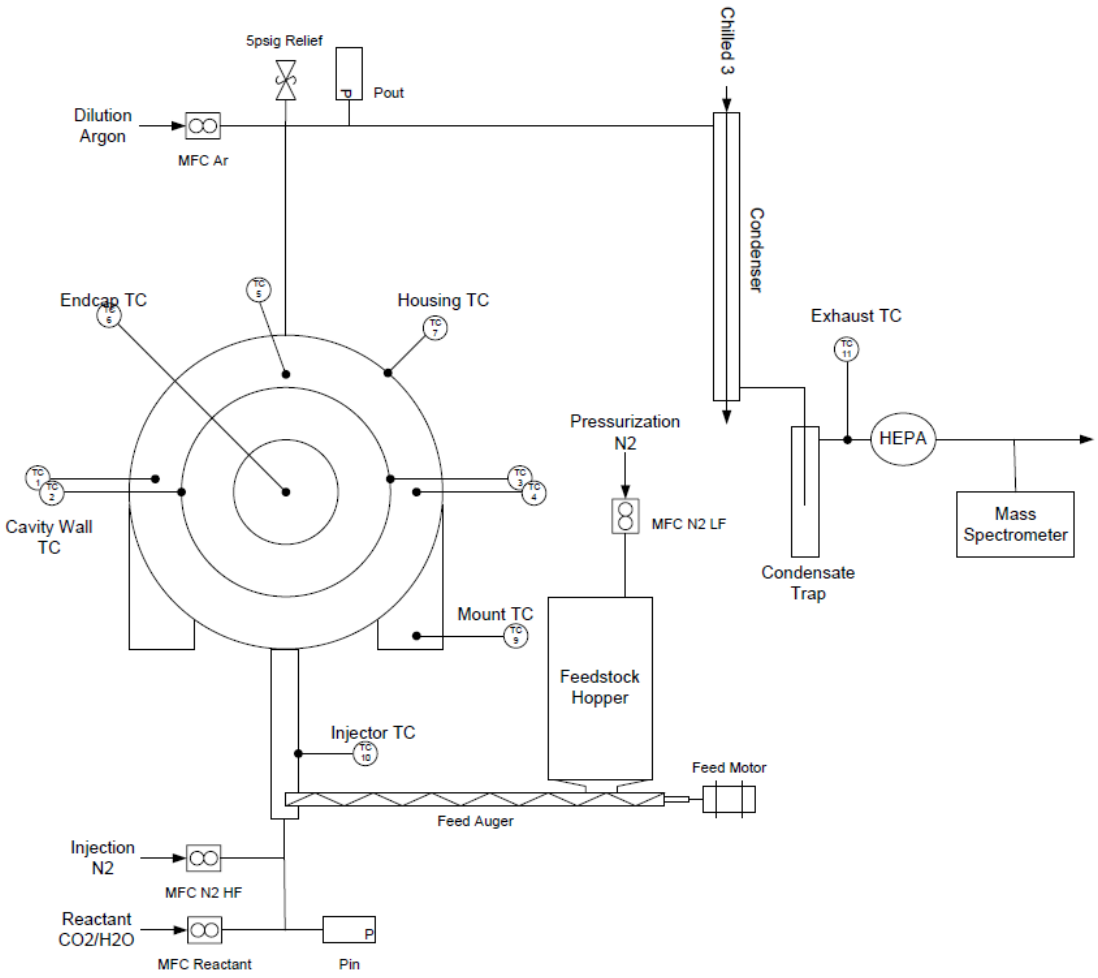

Figure 7.1 Location of sensors on reactor assembly

7.2 Implementation

The Labview VI written has a front panel and block diagram. Front panel is GUI which lets the user monitor the real time output of various sensors. Block diagram has the code which is the functional unit of the VI. Front panel and block diagram are represented in fig 7.2 and fig 7.3 respectively.

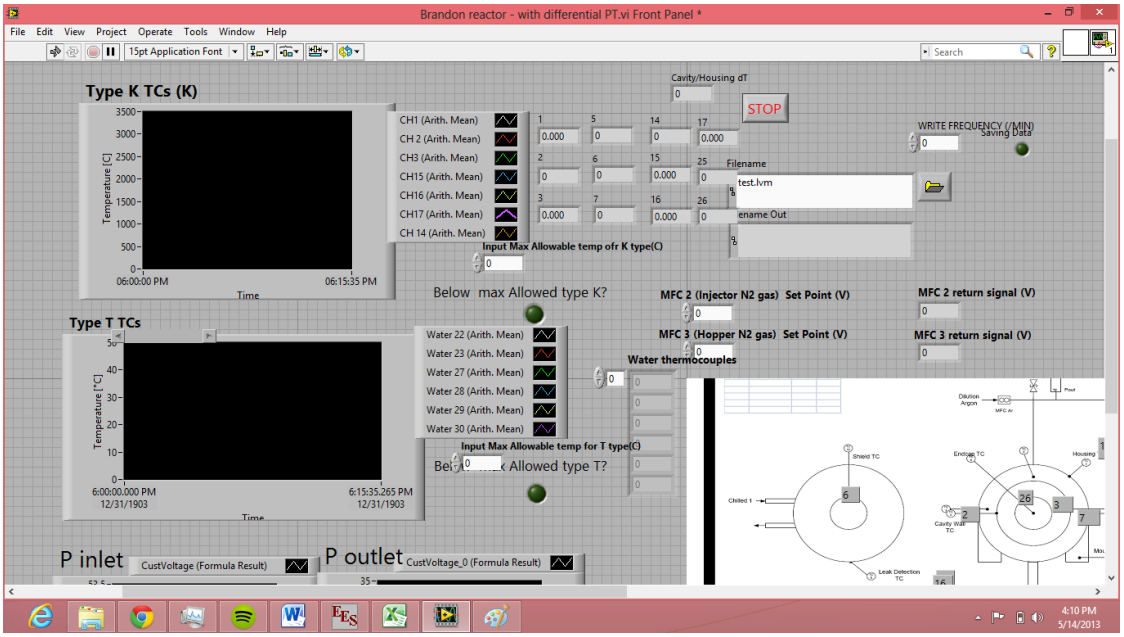

Figure 7.2 Front panel of Labview

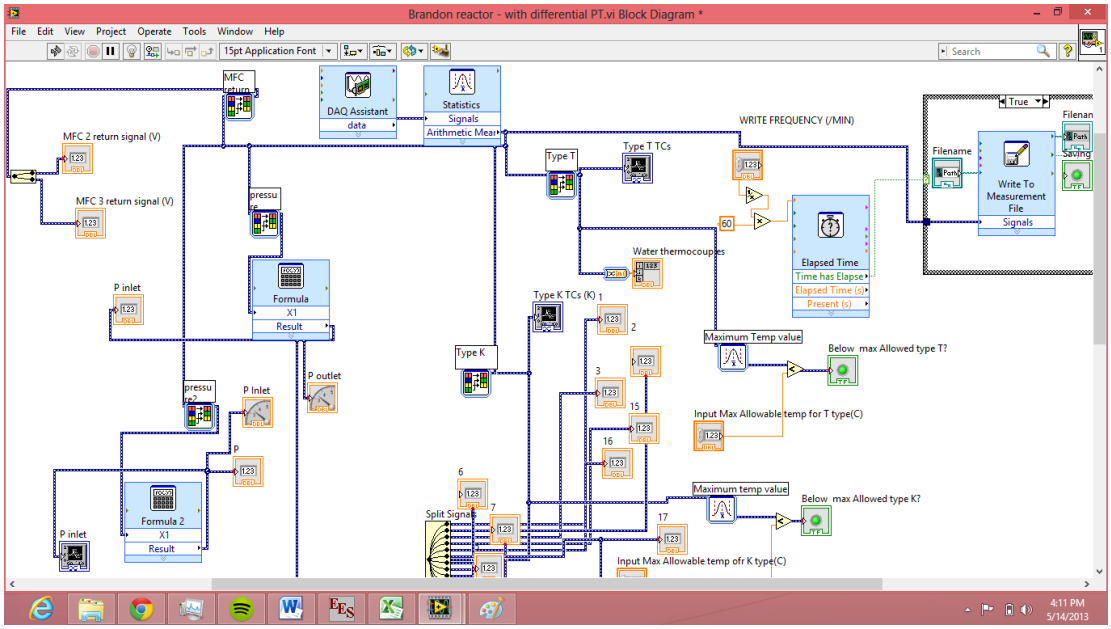

Fig 7.3: Block diagram of the Labview

8. Conclusions and Recommendations for Further Study

8.1 Conclusion

The present study focuses on design, fabrication and calibration of a feedstock delivery system for a 3kW prototype solar gasification reactor. The primary objective of the study was to fabricate a feed delivery system capable of delivering 8±(0.4) gm/min to 15±(0.75) gm/min. of cellulose powder to a gasification reactor. The most challenging aspect of the study was to select a proper conveying device. Since commercial augers are made mostly in large sizes (>2" diameter) and are not available in the small size that was determined taking into the required volumetric flow rate of feed material, a simple deep drill wood bit was selected as a screw feeder. Another challenging part of the study was to design a feed injector. The opening of the flow passage in the feed injector was optimized after taking into account the feed particle size and manufacturing feasibility. Large flow passage, although would be required for considerably larger feed particles or any foreign particle of abnormally large size, but it would have decreased the thermal efficiency of the reactor due to large flow of N_2 going to the reactor.

Testing was carried out to produce calibration of feed mass flow rate vs RPM of stepper motor. Overall, no overtorque condition or clogging was observed. Also repeatability was observed in terms of feed delivery rate as a function of RPM of the stepper motor. Calibration resulted in $\dot{m}_{feed} = (0.79 \pm 0.07)RPM - (7.32 \pm 2)$; 95% CI.

During the test of the feed delivery with the reactor, feed particles were delivered to the reactor for six minutes of time window. However, after that the pressure built up in the reactor due to the filters loading up with char. It caused the feed injector flow of N_2 to decrease to the point that entrainment of feed particles was no longer possible.

8.2 Recommendations for further study

The present experimental study mainly focuses on the cellulose particles as a feedstock which has a particle size of 0.5 mm. The design of various components of the feed system is done taking into account the size and mechanical properties of the cellulose particles. Although the change of feed material will not affect the hopper design that much, it will affect the feed injector flow passage area. Thus current feed delivery system is restricted to feed material with particle size about 0.5 mm or less. The stepper motor selected for the present study is based on torque requirement which depends upon the feed material mechanical properties and feed mass flow rate. Change of feed material might cause reconsideration for sizing the stepper motor. This issue can be addressed by replacing current stepper motor (NEMA size 23) by oversized stepper motor (NEMA size 34) which can be used for variety of feed material. To prevent the clogging of the feed material, screw feeder tube was cooled using air jet impingement. Although this method is effective, a better way could be water jacketing screw feeder tube.

The current feed delivery system does not provide any indication of level of feedstock in the hopper when experiment is going on. This can be improved by incorporating an acrylic window slot in the hopper wall to indicate the level of feedstock. Also to ensure that stepper motor is rotating at set RPM, an encoder can be employed to track the rotations of the stepper motor.

References

[1] Hathaway, B. J., 2013, "Solar Gasification of Biomass", Ph.D. thesis, Department of Mechanical Engineering, University of Minnesota.

[2] Dai, J., 2007, "Biomass Granular Feeding for Gasification and Combustion", Ph.D. thesis, Department of Mechanical Engineering, University of British Columbia.

[3] Zareiforoush, H., Komarizadeh, M. H., Alizadeh,M. R., and Masoomi, M., "Screw Conveyer Power and Throughput Analysis During Horizontal Handling of Paddy Grains", Journal of Agricultural Science,2(2),pp. 1.

[4] Srivastava, A. K., Goering, C. E., Rohrbach, R. P., and Buckmaster, D. R., 2006, *Engineering Principles of Agricultural Machines*, Second Edition, ASABE, pp: 491-524.

[5] Structure of a screw conveyer. Retrieved from: http://toritdust.com/parts/auger_conveyors.htm.

[6] Types of flights. Retrieved from: http://www.kaseconveyors.com/bulk-material-handling-products/engineering-guide/conveyor-flight-pitch-types.htm.

[7] Colijn, H., 1985, *Mechanical Conveyers for Bulk Solids*, Elsevier, New York, NY, Chap. 3.

[8] *Gravity Flow of Bulk Solids*, 1964, University of Utah Engineering Experiment Station, Bulletin 108.

[9] Chase, G. G., 2004, *SOLIDS NOTES 10*, The University of Akron.

[10] Rhodes, M., 1998, *Introduction to Particle Technology*, John Wiley and Sons, West Sussex, England, Chap.10.

[11] Roberts, A.W., 2002, "Design considerations and performance evaluation of screw conveyors", Bulk Solids Handling, 22, pp. 436-444.

[12] Schematic of deep hole drill bit. Retrieved from: http://www.mcmaster.com/#drill-bits-for-wood/=nhwvij.

[13] Torque vs speed characteristics for NI NEMA 23 stepper motor. Retrieved from: http://sine.ni.com/ds/app/doc/p/id/ds-311/lang/en.

[14] Rhodes, M., 1998, *Introduction to Particle Technology*, John Wiley and Sons, West Sussex, England, Chap.8.

[15] Arastoopour, H., Modi, M.V., Punwani, D.V., Talwalkar, A.T., 1979 "Review of design equations for dilute phase gas-solids horizontal conveying systems for coal and related materials", *The Power and Bulk Solids Conference*.

[16] Kays, W. M., Crawford, M. E., and Weigand, B., 2004, *Convective Heat and Mass Transfer*, 4th ed., McGraw-Hill.

[17] Incropera, F. P., and DeWitt, D. P., 2007, *Fundamentals of Heat and Mass Transfer*, John Wiley and Sons, pp.557.

[18] Internal friction data for various materials. Retrieved from: http://www.stanford.edu/~tyzhu/resources.htm

[19] Beverloo, W. A., Leniger, H.A., Van de Velde, J., 1961 "The Flow of Granular Solids Through Orifices", Chem Eng Sci, 115, pp. 260-269.

Appendix A

EES code to obtain volume flow rate of nitrogen gas in feed injector:

EES code

```
Tgas=100+ 273
Pgas=101325+ 27000
TSTP=273

rhog=density('Nitrogen',T=Tgas,p=Pgas)
rhop=1200
D=0.12*2.54/100
D_tube=0.18*2.54/100
A_tube=3.14*0.25*D_tube^2
A_tube*V_tube=A*Usafe
L_tube=72*2.54/100
g=9.8
mu=viscosity('N2',T=Tgas)
Mp=15/60/1000
A=3.14*0.25*D^2
Gp=Mp/A

Ut=(2*rp)^2*(rhop-rhog)*g/(18*mu)

((Uch/e)-Ut)=Gp/(rhop*(1-e))
rhog^(0.77)=2250*D*(e^(-4.7)-1)/((Uch/e)-Ut)^2
Usafe=1.5*Uch
VolumeSTP=1000*60*A*Uch*TSTP/Tgas

safeVolume=1.5*VolumeSTP


Uf=Usafe/e
Up=(Mp/rhop)/(A*(1-e))

//Pressure drop calculation

F_fw=(4*tau_w*L/D)
```

(c_f)/2=0.023*Re^(-0.2)

c_f=(tau_w)/(0.5*rhog*Uf^2)

Re=rhog*Uf*D/mu
L=80/1000

F_pw=0.057*Gp*L*(g/D)^0.5

T1=0.5*rhog*e*Uf^2
T2=0.5*(1-e)*rhop*Up^2
T3=F_fw*L
T4=F_pw*L
T5=rhop*L*(1-e)*g
T6=rhog*L*e*g

delta_P=T1+ T2+ T3+ T4+ T5+ T6

Pressuredrop =delta_P

// Pressure head

// Change Ps by supply line pressure-pressure drop in the line from gas cylinder to feed injector

Ps=101325
P_dyn=Pgas*(0.028*0.5*Uf^2)/(8.314*Tgas)
P_total=Ps+ P_dyn

P_ratio=P_dyn/P_total

// Pressure drop in supply line

F_fw_tube=(4*tau_wtube*L_tube/D_tube)

(c_ftube)/2=0.023*Re_tube^(-0.2)

c_ftube=(tau_wtube)/(0.5*rhog*V_tube^2)

Re_tube=rhog*V_tube*D_tube/mu

T1_tube=0.5*rhog*V_tube^2

T3_tube=F_fw_tube*L_tube

T6_tube=rhog*L_tube*g

delta_P_tube=T1_tube+ T3_tube+ T6_tube

Pressuredrop_total=delta_P_tube+ delta_P

// Friction factor asumption

// flow in tube is laminar based on Reynolds number criteria
f=64/Re_tube

deltaP_friction =f*(L_tube/D_tube)*(0.5*rhog*V_tube^2)

Appendix B

Standard Operating Procedure (SOP) for feedstock delivery system

<u>Follow the steps in the given order:</u>

Initial system check:

1. for gas system

- Check N2 cylinder for sufficient N2 quantity (300 psig) as per required test run time.
- Ensure gas lines connecting to MFC are leak free and located such that it can NOT be obstructed due to someone stepping over.
- Ensure same for gas lines connecting from MFC to hopper and feed injector.

2. Electronics and Power supply

- Make sure that there will not be any power shut down during test run.
- The computer used for running NI MAX (package for stepper motor) is working. Deactivate auto sleep/power saver mode of PC
- All wires connecting from stepper drive to stepper motor are intact and well insulated.
- Thermocouples monitoring the temperatures of feed injector and screw tubing are intact.

3. Clogging check

- Check screw feeder and hopper thoroughly for any residual clogging from last run.
- Thoroughly clean the screw and screw tubing so that no residual feedstock is left from last test run.

4. Assembly check

Once screw tubing is checked for residual feedstock, assemble the system and ensure that required protrusion of screw into feed injector opening. (This can be checked by holding lit torch below feed injector and seeing the protrusion)

- The coupling screws should be tightly held on motor shaft and screw shaft to prevent relative slippage between two shafts.
- Load the hopper with required quantity of feedstock.

5. Leak Check

- Ensure that all tube fitting connections are tight and leak free.
- Also once the hopper is loaded with feedstock, ensure that gasket is in place and all screws are tight to maintain pressurized hopper.
- Check for the bearing for any leaks.

Once above mentioned criteria are checked, you can now proceed with starting the system.

1. Start cooling system (air jets) to feed injector
2. Start Feed injector gas flow (4.2 SLPM which corresponds to 2.2 V signal input to MFC2) and then hopper gas flow (200 ccm).
3. Start the NI MAX program to start stepper motor.
4. Check the direction of rotation of stepper motor to ensure forward feeding into reactor. If direction is reverse, either power off stepper motor system and interchange A+ and A- on stepper drive then plug in or set the target position to 9999999. Forward direction can be ensured by looking at the velocity indicator on MAX. If it shows positive number, it means direction is correct.
5. Monitor the temperatures continuously along screw tubing once preheating of the reactor is started using tape heaters and ensure that compressed air jet flow is sufficient to keep the joint between feed injector and screw tubing is just

above saturation temperature for steam and temperature of screw tubing directly below hopper is maintained sufficiently cooler.

6. Start stepper motor by setting at 22 RPM (obtained from calibration) and solar simulator at the same time For 11 gm/min of feed delivery rate, set RPM of stepper motor to 22 and acceleration and deceleration to 5 rps/s.
7. When above steps are implanted, feed system is delivering feedstock to the reactor at required mass flow rate.

Stopping the feedstock system:

When required amount of test run is done, the feedstock delivery system needs to be stopped.

1. Decelerate stepper motor using NI MAX program to stop it.

2. Increased the compressed air jet flow rate at joint to bring down its temperature rapidly to near room temperature. If this is not done, residual feedstock in tube near joint will start clogging. Although this is not a serious problem, but it means more cleaning will be required for preparing feedstock delivery system for next text run.

3. Do not stop the N_2 supply to feed injector and hopper until molten salt is drained out from reactor and leftover salt in rector is at a temperature lower than its melting point.

4. Once the system is cooled completely, open the hopper and remove any leftover feedstock.

Appendix C

Failure modes

Introduction:

Failure Mode Analysis (FMA) has been carried out for various components of the feedstock delivery system. It briefly describes the failure modes possible for each component along with its potential cause and possible effects. FMA enables user to foresee any possible failure based on observation/ sensors output (as described below. It also suggests the remedial measures so that failed component can be fixed.

Table C.1: Failure modes

Component	**Failure mode**	**Possible Effects**	**Potential causes**	**Fix**
Feedscrew	1.Solid feedstock clogs inlet passage	Feeding stops. Salt temperature begins to rise. Salt backflow into feed injector. Line pressure upstream of clog begins to rise.	Excessive feed rate. Insufficient gas to feed rate.	Slow feedstock delivery rate. Increase vertical injection path diameter
	2.Char/tar clogs inlet passage	Feeding stops. Salt temperature begins to rise. Salt backflow into feed injector. Line pressure upstream of	Excessive Injector temperature. Excessive solid residence time in injector.	Increase cooling of injector body
	3.Loss of gas flow			Ensure sufficient

		clog begins to rise. Feedstock fills injector body and feeding stops. Salt backflow into feed injector.	Insufficient gas supply line pressure. Insufficient gas flow setpoint applied to MFC.	nitrogen available before experiment.
Feedscrew	Loss of feed flow	Salt temperature begins to rise.	Stepper motor failure or overtorque condition. Feedstock in solid rotation with shaft (no feeding).Motor to screw shaft to coupling failure. Labview freezes.	Check stepper motor wiring. Increase motor size if required. Switch from auger based to helical spring based feeding. Make sure that coupling screws are tight so that there is no relative motion between motor shaft and screw shaft.
Hopper	Feedstock bridging over feedscrew. Loss of gas seal	Loss of feed flow as described above Backflow of gas from injector. Inability to carry feed into	Feedstock too moist. Hopper walls too flat Bearing seal failure. Tube fitting seal failure. Hopper	Add hopper vibration. Consider further drying feedstock. Make sure that sight glass is clean Perform leak checks. Replace failed seals. Consider new

	Loss of pressurization	reactor. Potential clogging of injector. Potential backflow of salt from rector to injector. Backflow of gas from injector. Inability to carry feed into reactor. Potential clogging of injector. Potential backflow of salt from rector to injector.	window seal failure. Hopper to tube welds failure. Insufficient gas supply pressure. Insufficient gas flow setpoint for MFC.	fitting or shaft bearing arrangement. Ensure sufficient nitrogen is available before testing. Ensure emergency air divergence valve available in case of loss of nitrogen supply. Check MFC setpoint.